(12) INTERNATIONAL APPLICATION PUBLISHED UNDER THE PATENT COOPERATION TREATY (PCT)

(19) World Intellectual Property Organization
International Bureau

(43) International Publication Date
20 January 2022 (20.01.2022)

WIPO | PCT

(10) International Publication Number
WO 2022/015462 A2

(51) International Patent Classification:
B01J 23/00 (2006.01)

(21) International Application Number:
PCT/US2021/037959

(22) International Filing Date:
17 June 2021 (17.06.2021)

(25) Filing Language: English

(26) Publication Language: English

(30) Priority Data:
63/040,513 17 June 2020 (17.06.2020) US

(71) Applicant: **ARIZONA BOARD OF REGENTS ON BEHALF OF ARIZONA STATE UNIVERSITY** [US/US]; SkySong, 1475 N. Scottsdale Rd., Suite 200, Scottsdale, Arizona 85257 (US).

(72) Inventors: **ZHOU, Chen**; 1624 E. Monterey St., Chandler, Arizona 85225 (US). **RITTMANN, Bruce**; 90 West Cottage Ln., Tempe, Arizona 85282 (US). **ZHOU, Dandan**; 2555 Jingyue Street, Changchun, Jilin 130117 (CN). **LUO, Yihao**; 1121 N. 44th St., #3091, Phoenix, Arizona 85008 (US). **LONG, Min**; 13021 S. 48th Street, Phoenix, Arizona 85044 (US). **ZHENG, Chenwei**; 1886 E. Don Carlos Ave., Unit 167, Tempe, Arizona 85281 (US).

(74) Agent: **FULLER, Rodney J.**; Booth Udall Fuller, PLC, 1255 W. Rio Salado Parkway, Suite 215, Tempe, Arizona 85281 (US).

(81) Designated States *(unless otherwise indicated, for every kind of national protection available)*: AE, AG, AL, AM, AO, AT, AU, AZ, BA, BB, BG, BH, BN, BR, BW, BY, BZ, CA, CH, CL, CN, CO, CR, CU, CZ, DE, DJ, DK, DM, DO, DZ, EC, EE, EG, ES, FI, GB, GD, GE, GH, GM, GT, HN, HR, HU, ID, IL, IN, IR, IS, IT, JO, JP, KE, KG, KH, KN, KP, KR, KW, KZ, LA, LC, LK, LR, LS, LU, LY, MA, MD, ME, MG, MK, MN, MW, MX, MY, MZ, NA, NG, NI, NO, NZ, OM, PA, PE, PG, PH, PL, PT, QA, RO, RS, RU, RW, SA, SC, SD, SE, SG, SK, SL, ST, SV, SY, TH, TJ, TM, TN, TR, TT, TZ, UA, UG, US, UZ, VC, VN, WS, ZA, ZM, ZW.

(84) Designated States *(unless otherwise indicated, for every kind of regional protection available)*: ARIPO (BW, GH, GM, KE, LR, LS, MW, MZ, NA, RW, SD, SL, ST, SZ, TZ, UG, ZM, ZW), Eurasian (AM, AZ, BY, KG, KZ, RU, TJ,

(54) Title: SYSTEMS FOR CATALYTICALLY REMOVING OXIDIZED CONTAMINANTS FROM A FLUID AND RELATED METHODS

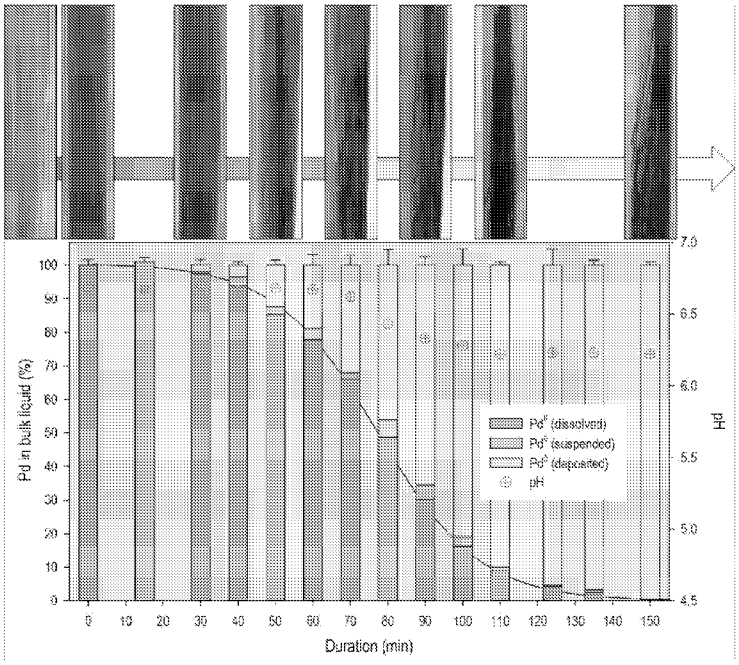


FIG. 2

(57) Abstract: The present invention relates to systems and methods for catalytic removal of oxidized contaminants (for example, nitrite, chromate, chlorate, trichloroethene, CFC-11, 4-nonylphenol, RDX, and perfluorooctanoate) from water and wastewater. In some aspects, the catalytic method of removing oxidized contaminants comprises using precious metal nanoparticles as catalysts to reduce the oxidized contaminants.

[Continued on next page]

WO 2022/015462 A2

TM), European (AL, AT, BE, BG, CH, CY, CZ, DE, DK, EE, ES, FI, FR, GB, GR, HR, HU, IE, IS, IT, LT, LU, LV, MC, MK, MT, NL, NO, PL, PT, RO, RS, SE, SI, SK, SM, TR), OAPI (BF, BJ, CF, CG, CI, CM, GA, GN, GQ, GW, KM, ML, MR, NE, SN, TD, TG).

Published:

— *without international search report and to be republished upon receipt of that report (Rule 48.2(g))*

SYSTEMS FOR CATALYTICALLY REMOVING OXIDIZED CONTAMINANTS FROM A FLUID AND RELATED METHODS

CROSS-REFERENCE TO RELATED APPLICATIONS

[0001] This application claims the benefit of and priority to U.S. provisional patent application 63/040,513, filed June 17, 2020, the entirety of the disclosure of which is hereby incorporated by this reference thereto.

STATEMENT REGARDING FEDERALLY SPONSORED RESEARCH OR DEVELOPMENT

[0002] This invention was made with government support under W912HQ-17-C-0013 awarded by the Army Research Laboratory. The government has certain rights in the invention.

FIELD OF THE INVENTION

[0003] The invention relates to systems and methods for removing oxidized contaminants from water or wastewater.

BACKGROUND OF THE INVENTION

[0004] Precious metal-based catalysis has emerged as a promising strategy for efficiently promoting destruction of a wide spectrum of oxidized contaminants in water via H_2-, borohydride-, or formate-induced reduction in ambient conditions. Its practical applications for long-term continuous treatment of water and wastewater at large scales, however, have not been realized due to two crucial roadblocks.

[0005] First, most laboratory-scale tests of catalytic contaminant removal used precious-metal-based catalysts supported on micro-size activated carbon, metal oxides, silica, or polymeric dispersers (for example, polyvinyl pyrrolidone (PVP) and metal-organic frameworks (MOFs)). The coating of precious metal nanoparticles (NPs) onto these supporters requires high temperature and/or high pressure and thus is energy-consuming. In addition, NP synthesis and the NP coating are usually two distinct steps, which leads to a low yield of harvested catalysts. Often, only a small portion of the precursor or synthesized NPs can be retained on the supporter for subsequent catalytic applications. Furthermore, these precious metals/supporter catalysts are mostly suspended or fluidized evenly in liquid phase and, thus, subject to being washed out in continuous operation.

[0006] Second, only a few electron donors (H_2, formate, and borohydride) are able to drive reduction reactions catalyzed by precious metals. H_2 is advantageous compared to the other two electron donors, because it is nontoxic, does not generate any secondary contamination or carbon footprint, and can be readily obtained at a reasonable cost. However, H_2 has low-solubility gas diffusion, which means that its diffusion through gas-liquid interfaces and then to the catalytic surface significantly slows the catalytic reaction. From a practical perspective, conventional gas transfer approaches, which involve bubbling, are not feasible at full-scale applications due to the significantly high cost (reflected by wasting of H_2 and energy) and off-gassing of combustible H_2.

[0007] Accordingly, systems and methods that can overcome the roadblocks of using precious metal-based catalysis to remove contaminants are needed.

SUMMARY OF THE INVENTION

[0008] The disclosure relates to methods related to the removal of oxidized contaminants water or wastewater via precious metal-based catalysis and to systems for the practice of such methods. In some aspects, the disclosure also relates to methods and systems for synthesizing precious metal nanocatalysts.

[0009] In some aspects, a method for establishing a catalyst film for long-term removal of oxidized contaminants from a fluid is disclosed. The method comprises providing a non-porous gas transfer membrane. The non-porous gas transfer membrane comprises a gas-phase side and a liquid-phase side. The method further comprises contacting the liquid-phase side of the non-porous gas transfer membrane with a precious metal medium and contacting the gas-phase side of the non-porous gas transfer membrane with hydrogen (H_2) gas at a sufficient partial pressure to convert at least 90% of the precious metal salt in the precious metal medium to elemental form. The precious metal medium comprising a precious metal salt and a solvent. The elemental form of the precious metal is in the form of a nanoparticle and is deposed on the liquid-phase side of the non-porous gas transfer membrane. In particular embodiments, the mean diameter of the precious metal nanoparticles is less than 5 nm.

[0010] In other aspects, a method for removing oxidized contaminants from a fluid is disclosed. The method comprises establishing a catalyst film comprising precious metal nanoparticles on a non-porous gas transfer membrane; contacting a fluid containing oxidized contaminant to the catalyst film; and contacting the catalyst film with H_2 gas, wherein the precious metal nanoparticles reduce the oxidized contaminants and the H_2 gas is provided at a sufficient partial pressure to reduce the oxidized contaminants.

[0011] In yet other aspects, a system for removing oxidized contaminants from a fluid is described. The system comprises a non-porous gas transfer membrane, a catalyst film comprising precious metal nanoparticles, and a H_2 gas source. The catalyst film is deposed on the non-porous gas transfer membrane. The precious metal nanoparticles and the hydrogen gas catalyze the reduction of oxidized contaminants. The catalyst film is deposed on the liquid-phase side of the gas transfer membrane, and the H_2 gas source delivers H_2 gas to the gas-phase side of the gas transfer membrane.

[0012] In some aspects, the catalyst film consists of precious metal nanoparticles. In particular embodiments, the catalyst film consists of precious metal nanoparticles with a mean diameter of less than 5 nm.

BRIEF DESCRIPTION OF THE DRAWINGS

[0013] FIG. 1 illustrates, in accordance with certain embodiments, a schematic of a bench-scale form of the catalytic reactor (also referred to herein as H_2-MCfR).

[0014] FIG. 2 depicts, in accordance with certain embodiments, autocatalytic monometallic palladium nanoparticles synthesis and coating on the nonporous polypropylene hollow fiber membranes in the membrane catalyst film reactor (MCfR). The upper portion depicts photos of the fiber section in one MCfR glass tube over time. The lower portion depicts the average percentage profile of palladium species over time in the MCfR.

[0015] FIGs. 3-A1 to 3-A5 depict, in accordance with certain embodiments, scanning transmission electron microscopy (STEM) images of Pd-films coated on the membranes 0.1 mM Na_2PdCl_4 as the precursor.

[0016] FIGs. 3-B1 to 3-B5 depict, in accordance with certain embodiments, STEM images of Pd^0-films coated on the membranes 1 mM Na_2PdCl_4 as the precursor.

[0017] FIGs. 3-C1 to 3-C5 depict, in accordance with certain embodiments, STEM images of Pd^0-films coated on the membranes 2 mM Na_2PdCl_4 as the precursor.

[0018] FIGs. 3-D1 to 3-D5 depict, in accordance with certain embodiments, STEM images of Pd^0-films coated on the membranes 5 mM Na_2PdCl_4 as the precursor.

[0019] FIG. 4 depicts, in accordance with certain embodiments, the reduction of nitrite catalyzed by Pd-film (0.1 mM Pd precursor) in H_2-MCfRs (left), the reduction of chromate catalyzed by Pd-film (0.1 mM Pd precursor) in H_2-MCfRs (middle), and the reduction of chlorate catalyzed by Pd-film (0.1 mM Pd precursor) in H_2-MCfRs (right).

[0020] FIGs. 5A-5D depict, in accordance with certain embodiments, reduction of trichloroethane (TCA) catalyzed by Pd-film in a MCfR (FIG. 5A), reduction of

trichlorofluroroethane (CFC-11) catalyzed by Pd-film in a MCfR (FIG. 5B), reduction of 4-nitrophenol (4-NP) catalyzed by Pd-film in a MCfR (FIG. 5C), and reduction of 1,3,5-trinitroperhydro-1,3,5-triazine (RDX) catalyzed by Pd-film in a MCfR (FIG. 5D).

[0021] FIGs. 6A-6G depict, in accordance with certain embodiments, rate constants, catalytic activities, and product selectivities of Pd-film-catalyzed reductions of various oxidized contaminants in the MCfR.

[0022] FIG. 7 depicts, in accordance with certain embodiments, results of continuous removal of TCA and TCE in a MCfR featuring Pd-film as the catalyst.

[0023] FIG. 8 depicts, in accordance with certain embodiments, the concentration changes of Pd(II) and Rh(III) in the precious metal medium during the establishment of the catalyst film.

[0024] FIGs. 9A-9D depict, in accordance with certain embodiments, the characteristics of a Pd/Rh catalyst film as shown from microscopy and spectroscopy images. FIGs. 9A and 9B show the morphology of cross sections of the Pd/Rh film (images from transmission electron microscopy). FIGs. 9C and 9D show diffraction patterns from electron energy loss spectroscopy, which show Pd^0 and Rh^0 are located on different planes of the catalyst film.

[0025] FIGs. 10A-10C depict, in accordance with certain embodiments, the removal and defluorination of PFOA by Pd/Rh-film and Pd/Ir-film at pH 7.

[0026] FIG. 11 depicts, in accordance with certain embodiments, the concentration of PFOA during continuous operation of a MCfR with a Pd/Rh-film.

DETAILED DESCRIPTION OF THE INVENTION

[0027] Detailed aspects and applications of the invention are described below in the drawings and detailed description of the invention. Unless specifically noted, it is intended that the words and phrases in the specification and the claims be given their plain, ordinary, and accustomed meaning to those of ordinary skill in the applicable arts.

[0028] In the following description, and for the purposes of explanation, numerous specific details are set forth in order to provide a thorough understanding of the various aspects of the invention. It will be understood, however, by those skilled in the relevant arts, that the present invention may be practiced without these specific details. It should be noted that there are many different and alternative configurations, devices, and technologies to which the disclosed inventions may be applied. The full scope of the inventions is not limited to the examples that are described below.

[0029] The singular forms "a," "an," and "the" include plural referents unless the context clearly dictates otherwise. Thus, for example, reference to "a step" includes reference to one or more of such steps.

[0030] The term "about" when used in the context of numeric values denotes an interval of accuracy that is familiar and acceptable to a person skilled in the art. The interval is ±10% of the given numeric value, ±5% of the given numeric value, or ±2% of the given numeric value.

[0031] As used herein, the term "precious metal" refers to gold (Au), silver (Ag), and platinum group metals (PGM). The members of PGM include platinum (Pt), palladium (Pd), ruthenium (Ru), rhodium (Rh), osmium (Os), and iridium (Ir).

[0032] As used herein, the terms "precious metal-film" and "catalyst film" refer to a film of precious metal nanocatalysts.

[0033] Disclosed herein is an innovative technology that features a sustainable nanoparticle support for catalytic reduction of oxidized contaminants to remove these contaminants from a fluid. The catalytic reactor system (H_2-MCfR) described herein have minimal catalyst loss and efficient gas delivery for maximal H_2 utilization. Accordingly, the disclosure also relates to methods for removing at least one oxidized contaminant from a fluid. The oxidized contaminants that can be removed by the disclosed system methods include herbicides, pesticides, disinfection byproduct, solvents, freon, explosives, and precursors or raw materials, for example, nitrite, chromate, and trichloroethene. In particular embodiments, the catalytic reactor system reduces at least one oxidized contaminant selected from the group consisting of: chlorophenols, 2,4-dichlorophenoxyacetic acid, 3,6-dichloro-2-methoxybenzoic acid, 1-chloro-3-ethylamino-5-isopropylamino-2,4,6-triazine, 3,5-dibromo-4-hydroxybenzonitrile, trichloroacetic acid, trichloroacetonitrile, NDMA, bromochloroiodomethane, trichloroethane, trichloroethene, chloroform, CFC-11, CFC-12, CFC-113, phenol, nitrophenols, PFAS, 1,3,5-Trinitro-1,3,5-triazinane, 1,3,5,7-Tetranitro-1,3,5,7-tetrazoctane, and TNT.

[0034] Compared to biological systems for treating oxidized contaminants, the catalytic reactor system described herein does not have a lag phase, is more stable, has no issues with fouling, and is more resistant against sudden changes of operational conditions. Additionally, no addition of organic electron donors, which may cause secondary contamination, are needed. The catalytic reactor system has significantly faster removal of organic contaminants compared to biological systems for treating oxidized contaminants.

[0035] Compared to other catalytic systems for treating oxidized contaminants, the disclosed catalytic reactor system enables one-pot synthesis and does not require high

temperatures or pressures. Accordingly, the energy and resource costs for the synthesis of catalysts are less for the catalytic reactor system described herein. The utilization of precursors in the disclosed catalytic reactor system is over 99%. The disclosed catalytic reactor system also treats a wider spectrum of contaminants than catalytic systems of the prior art. As shown in the example, the catalytic system described herein is suitable for long-term continuous treatment, as it has minimal catalyst loss and constantly high catalytic activity.

Catalytic Reactor System

[0036] The catalytic reactor system comprises a film of precious metal nanoparticles (the catalyst film), a gas transfer membrane on which the film of precious metal nanoparticles is deposed, and a hydrogen-gas source. In some embodiments, the gas transfer membrane is nonporous. H_2 gas is delivered to the lumen at a carefully controlled pressure, and the H2 diffuses through the walls in a bubbleless form. The H_2 gas functions as the electron donor to drive autocatalytic reduction of the soluble precious metals (with an oxidation state of +2 or +3) to elemental precious metals (with an oxidation state of 0), which spontaneously deposit as nanoparticles on the membrane wall of the liquid-phase side. The H_2 gas also facilitates the reduction of oxidized contaminants by the precious metal nanoparticles. Accordingly, "precious metal nanocatalyst" as referenced herein refer to the film of precious metal nanoparticles deposed on the gas transfer membrane. A bench-scale example of this system is shown in FIG. 1.

[0037] In particular embodiments, the catalyst film is spontaneously formed on the liquid-phase side of the gas transfer membrane, for example, the member's outer surfaces, which would be the liquid-phase side. The liquid-phase side of the gas transfer membrane is in fluid contact with the liquid containing precious metal contaminants or a precious metal medium. For example, dissolved Pd(II) in the precious metal medium is autocatalytically reduced by the H_2 gas provided by the hydrogen-gas source to form Pd^0 nanoparticles (NPs) that are simultaneously deposited on the gas transfer membrane as a Pd^0-film. The Pd^0-film is capable of catalyzing the oxidation of the H_2 coupled to reduction of the oxidized contaminants in the bulk liquid. As another non-limiting example, a precious metal medium containing dissolved Pd(II) and Rh(III) is contacted to the liquid-phase side of the gas transfer membrane, and the H_2 gas provided by the hydrogen-gas source facilitates the reduction of Pd(II) and Rh(III) to Pd^0 and Rh^0. The Pd^0 and Rh^0 nanoparticles are simultaneously deposited on the gas transfer membrane as a Pd/Rh-film.

[0038] Thus, described herein is a method of producing the catalyst film. The method comprises providing an aqueous system in contact with a nonporous gas transfer membrane; submerging the nonporous gas transfer membrane in a precious metal medium; and pressurizing the gas-phase side of the membrane with H_2 at desired partial pressure, wherein precious metal nanoparticles are formed and coated on the nonporous gas transfer membrane to form a catalyst film. Thus, in some aspects, the catalyst film consists of precious metal nanoparticles. In certain embodiments, the catalyst film consists of nanoparticles of one type of precious metal, which is also referred to herein as a monometallic catalyst film. In other embodiments, the catalyst film consists of nanoparticles of two types of precious metals, which is also referred to herein as a bimetallic catalyst film.

[0039] In some aspects, the method comprises contacting the liquid-phase side of the gas transfer membrane with a precious metal medium. Meanwhile, the gas-phase side of the non-porous gas transfer membrane is contacted with H_2 gas at a sufficient partial pressure to convert at least 90% of the precious metal salt in the precious metal medium to elemental form. In some aspects, at least 99% of the precious metal salt in the precious metal medium is converted to elemental form. In particular implementations, at least 90% of the precious metal salt in the precious metal medium is converted to elemental form within 150 minutes of contact with the precious metal medium and H_2 gas. In certain implementations, at least 90% of the precious metal salt in the precious metal medium is converted to elemental form within 110 minutes of contact with the precious metal medium and H_2 gas. In some aspects, at least 99% of the precious metal salt in the precious metal medium is converted to elemental form within 150 minutes of contact with the precious metal medium and H_2 gas. In a particular embodiment, at least 99% of the precious metal salt in the precious metal medium to is converted elemental form within 110 minutes of contact with the precious metal medium and H_2 gas. In certain embodiments, the elemental form of the precious metal are nanoparticles with a mean diameter of less than 5 nm, less than 4 nm, less than 3 nm, less than 2 nm, less than 1 nm, less than 0.5 nm, or between 0.3 nm and 0.4 nm. In some embodiments, the precious metal nanoparticles have diameters of less than 10 nm, for example, less than 9 nm, less than 8 nm, less than 7 nm, less than 6 nm, less 5 nm, less than 4 nm, less than 3 nm, less than 2 nm, less than 1 nm, less than 0.5 nm, or between 0.3 nm and 0.4 nm. In some aspects, the nanoparticles agglomerate to form nanoclusters, which have diameters of less than 10 nm, for example, less than 9 nm, less than 8 nm, less than 7 nm, less than 6 nm, less 5 nm, less than 4 nm, less than 3 nm, or less than 2 nm. Accordingly, in certain implementations, the catalyst film consists of precious metal nanoparticles with diameters of less than 10 nm, for example, with a mean diameter of less

than about 10 nm, less than about 9 nm, less than about 8 nm, less than about 7 nm, less than about 6 nm, less than about 5 nm, less than about 4 nm, less than 3 nm, less than 2 nm, less than 1 nm, less than 0.5 nm, or between 0.3 nm and 0.4 nm. In some aspects, the catalyst film consists of precious metal nanoparticles with a mean diameter of less than 5.5 nm, less than 5.25 nm, less 5 nm, less than 4.5 nm, less than 4.25 nm, less than 4 nm, less than 3.5 nm, less than 3.25 nm, less than 3 nm, less than 2.5 nm, less than 2.25 nm, less than 2 nm, less than 1.5 nm, less than 1.25 nm, less than 1 nm, less than 0.5 nm, less than 0.4 nm, or between 0.3 nm and 0.4 nm. In certain embodiments, the catalyst film comprises nanoclusters having diameters of less than 10 nm, for example, less than 9 nm, less than 8 nm, less than 7 nm, less than 6 nm, less 5 nm, less than 4 nm, less than 3 nm, or less than 2 nm.

[0040] In some aspects, the loading density of the catalyst film is between 5 mg and 12 g precious metal/m^2. For example, in certain embodiments, the loading density of a monometallic catalyst film is about 0.07 mmol Pd/m^2 (about 7.7 mg Pd /m^2) or 0.07 ± 0.007 mmol Pd/m^2 (7.7 ± 0.08 mg Pd/m^2). In other embodiments, the loading density of a bimetallic catalyst film is about 12 mg precious metal/m^2 or between 11 mg precious metal/m^2 to 11.5 mg precious metal/m^2. For example, the loading density of a Pd/Rh-film is 11.2 g precious metal/m^2, in particularly 5.6 g Pd/m^2 and 5.6 g Rh/m^2.

[0041] Accordingly, in certain embodiments, the catalytic reactor system further comprises a precious metal medium, which comprises at least one precious metal salt in a solvent. The precious metal medium provides the charged precious metal ions for the formation of the catalyst film on the gas transfer membrane. In some aspects, the precious metal medium the liquid containing precious metal contaminants, for example liquid from a waste stream that comprises precious metal contaminants.

[0042] The operational conditions of the catalytic reactor system can be conveniently and accurately tuned for optimizing the conditions to reduce particular oxidized contaminants. For example, the selection of particular precious metal and their amount in the precious metal medium for the production of the catalyst film, the pH in the liquid comprising the oxidized contaminants or the precious metal medium, H_2 pressure, and surface-loading rate of the oxidized contaminant each may be adjusted to optimize conditions for catalytic reduction of certain oxidized contaminants.

a. Gas Transfer Membrane:

[0043] The gas transfer membrane used in the catalytic reactor system does not have pores in its wall (for example, a nonporous membrane). The lack of pores in the membrane enables

transferring gas (for example, hydrogen) in a bubble-free form at controllable rates. In some embodiments, the membrane is a hollow-fiber membrane. In such embodiments, gas is supplied to the lumen of the hollow-fiber membrane (the gas-phase side). Accordingly, catalyst film would be anchored to the outer surface of the hollow-fiber membrane (the liquid-phase side). In other embodiments, the membrane is a flat- or curled-sheet membrane. In such embodiments, hydrogen gas is supplied to one side of the sheet membrane (the gas-phase side), while catalyst film is anchored to the other surface of the sheet membrane (the liquid-phase side).

[0044] The membrane may be made of a variety of polymeric materials, for example polypropylene, polyurethane, polysulfone, or composite forms. In certain embodiments, the thickness of the gas transfer membrane is may be 50-70 μm, for example between 50-55 μm.

[0045] In particular embodiments, the gas transfer membrane is a nonporous polypropylene hollow-fiber membrane (200 μm OD, 100-110 μm ID, wall thickness 50-55 μm).

b. Precious metal medium

[0046] Exemplary precious metals that could be used for producing the catalyst film include transition metal and post-transition metals. Example of transition metals that may be used to produce catalyst films include metals in the platinum metal group (which are ruthenium, rhodium, palladium, osmium, iridium, and platinum), copper, gold, silver, rhenium, molybdenum, wolframium, cobalt, and nickel. Examples of post-transition metals that may be used to produce catalyst films include tin, gallium, and indium.

[0047] The precious metal medium comprises a precious metal a solvent. The solvent in the precious metal medium is selected from at least one of water, salt solution, hydrochloric acid, methanol, ethanol, acetonitrile, toluene, dichloromethane, chloroform, or tetrahydrofuran. In certain implementations, the solvent is deionized water.

[0048] Precious metal salts rapidly dissolve in the solvent and release soluble precious metal ions. Soluble precious metal ions include Au^{3+}, Ag^{+}, $(PtCl_4)^{2+}$, $(PdCl_4)^{2+}$, Rh^{3+}, Ru^{3+}, Ir^{4+}, Os^{4+}, Cu^{2+}, Sn^{2+}, Ni^{2+}, Mo^{6+}, and W^{6+}. Accordingly, the precious metal medium comprises at least one precious metal ions selected from the group consisting of Au^{3+}, Ag^{+}, $(PtCl_4)^{2+}$, $(PdCl_4)^{2+}$, Rh^{3+}, Ru^{3+}, Ir^{4+}, Os^{4+}, Cu^{2+}, Sn^{2+}, Ni^{2+}, Mo^{6+}, and W^{6+}. Exemplary precious metal salts in the precious metal medium include gold chloride ($AuCl_3$), silver nitrate ($AgNO_3$), sodium tetrachloropalladate (Na_2PtCl_4), sodium tetrachloropalladate (Na_2PdCl_4), ruthenium chloride ($RhCl_3$), ruthenium chloride ($RuCl_3$), potassium hexachloroiridate (K_2IrCl_6), potassium hexachloroosmate (K_2OsCl_6) cupric chloride ($CuCl_2$), tin chloride ($SnCl_2$), nickel chloride ($NiCl_2$), molybdenum oxide (MoO_3), and sodium tungstate (Na_2WO_4).

[0049] The range of the concentration of the precious metal in the precious metal catalyst is wide, for example, 0.1-100 mM. In some aspects, the concentration of precious metal in the precious metal medium is 0.1-5 mM, for example 1-5 mM. In particular embodiments, the concentration of precious metal in the precious metal medium is about 0.1 mM, about 1 mM, about 2 mM, or about 5 mM. In some aspects, the concentration of precious metal in the precious metal medium is 0.1 ± 0.01 mM, 1 ± 0.1 mM, 2 ± 0.2 mM, or 5 ± 0.05 mM. In other aspects, the concentration of precious metal in the precious metal medium is 0.1 ± 0.005 mM, 1 ± 0.05 mM, 2 ± 0.1 mM, or 5 ± 0.025 mM.

[0050] In some embodiments, the precious metal medium further comprises an acid, a base, and/or pH buffers. The acid may be hydrochloric acid. The base may be sodium hydroxide. In particular embodiments, the pH buffer adjusts the pH of the precious metal medium to anywhere in the range of 0 and 14. In certain embodiments, the pH of the precious metal medium is between 3 and 10, for example, a pH of 3-8, 3.5-7.5, 6.5-8.5, or about 7. In some aspects, the pH of the precious metal medium is 7 ± 0.5, 7 ± 0.4, 7 ± 0.3, 7 ± 0.2, 7 ± 0.1, or 7 ± 0.05.

e. Hydrogen gas source

[0051] The hydrogen gas source can be any reliable source of H_2 gas, for examples, a gas storage tank having pressurized H_2 gas, a H_2 generator via water electrolysis, or a methane reformer. In some embodiments, the H_2 purity is over 99%. In other embodiments, the H_2-gas source include a built-in or external gas pressure regulator. The gas pressure regulator regulates the pressure of H_2 gas from the gas storage tank to the gas-phase side of the membrane. In particular implementations, the gas pressure regulator regulates the pressure of H_2 gas so that H_2 gas is delivered to the gas-phase side of the membrane at no more than about 30 psig, for example, 3-30 psig, 5-30 psig, 2-15 psig, 2.5-15 psig, 2-10 psig, between about 3 psig and about 9 psig, or at about 10 psig. In some embodiments, the gas pressure regulator regulates the pressure of H_2 gas so that H_2 gas is delivered to the gas-phase side of the membrane at a partial pressure of 2.7-9.9 psig, 10 ± 1 psig, 10 ± 0.5 psig, or 10 ± 0.25 psig.

[0052] In some aspects, the partial pressure of H_2 gas provided that is sufficient to convert at least 90% of the precious metal salt in the precious metal medium to elemental form within 150 minutes of contact with the precious metal medium and H_2 gas is about 10 psig, for example, 10 ± 1 psig, 10 ± 0.5 psig, or 10 ± 0.25 psig.

[0053] In some aspects, the partial pressure of H_2 gas provided to the catalytic reactor system is between 2 psig and 20 psig. In certain implementations, the partial pressure of H_2 gas

provided to the gas transfer membrane for reducing oxidized contaminants is between about 3 psig and about 5 psig, for example, about 3 psig, 3 ± 0.3 psig, about 4 psig, 4 ± 0.4 psig, or about 5 psig or 5 ± 0.5 psig. In some implementations, the partial pressure of H_2 gas provided for forming a monometallic catalyst film is between 2 psig and 10 psig, between about 3 psig and about 9 psig or 2.7-9.9 psig. In some implementations, the partial pressure of H_2 gas provided for forming a bimetallic catalyst film and for reducing oxidized contaminants is between 10 psig and 20 psig.

Methods of removing oxidized contaminants from a fluid

[0054] The described methods of removing oxidized contaminants from a fluid comprises catalytically converting the contaminants into harmless or readily biodegradable forms. In some aspects, the methods of catalytically reducing oxidized contaminants described herein do not result in catalyst loss. The method comprises providing a fluid comprising an oxidized contaminant to the catalyst film, where the catalyst film reduces the oxidized contaminant. In some implementations, the method comprises tuning operational conditions of the catalytic reactor system to optimize treatment efficiency (for example, maximizing the contaminant removal rate and minimizing undesired products). In some aspects, the operational conditions are adjusted to ensure there is little to no catalyst loss.

[0055] In particular implementations, method comprises establishing a catalyst film comprising precious metal nanoparticles; contacting a fluid containing oxidized contaminant to the catalyst film; and contacting the catalyst film with hydrogen (H_2) gas. The precious metal nanoparticles reduce the oxidized contaminants and the H_2 gas is provided at a sufficient partial pressure to reduce the oxidized contaminants. In some aspects, the fluid containing the oxidized contaminants is water or wastewater.

[0056] As shown in the examples, the optimal partial pressure of H_2 gas provided reduce a large variety of oxidized contaminants via a monometallic catalyst film is 2-10 psig, between about 3 psig and about 9 psig, 2.7-9.9 psig, between about 3 psig and about 5 psig, for example, about 3 psig, 3 ± 0.3 psig, about 4 psig, 4 ± 0.4 psig, or about 5 psig or 5 ± 0.5 psig.

Illustrative, Non-Limiting Examples in Accordance with Certain Embodiments

[0057] The disclosure is further illustrated by the following examples that should not be construed as limiting. The contents of all references, patents, and published patent applications cited throughout this application, as well as the figures, are incorporated herein by reference in their entirety for all purposes.

1. Activation of MCfR: forming Pd^0-film

[0058] A bench-scale MCfR featuring monometallic a Pd^0-film was prepared in ambient conditions (23°C and 1 atm). The MCfR was of the same dual-tube design as shown in FIG. 1. The working volume of the MCfR was 60 mL. One bundle of 60 25-cm polypropylene fibers was installed in each of the dual tubes, giving a total membrane surface of 190 cm^2. The liquid phase of the MCfR was filled with Pd^{2+} medium. The Pd^{2+} medium contains 600 mg/L sodium tetrachloropalladate (Na_2PdCl_4; i.e., 2.0 mM soluble Pd(II)) as the precursor. The pH of the medium was adjusted to 7. H_2 was supplied from a pure-H_2 tank at a constant partial pressure of 10 psig.

[0059] FIG. 2 shows photos of a fiber section and the concentration profile of the Pd species over time in one MCfR. The first 40 minutes involved nucleation, and only 6% of the soluble Pd(II) was reduced to insoluble Pd^0. By eighty minutes, more than one-half of the total added Pd(II) was deposited on the fiber surface at Pd^0, turning the fibers' color from white to greyish-black. Then, Pd(II) reduction accelerated, with more than 99% of the total Pd converted to Pd^0 by 110 minutes, and the fibers turned dark black, since the reduced Pd^0 solids were deposited onto the fiber surface. Full reduction to Pd^0 and its deposition on the fibers were further confirmed by the minimal concentrations of insoluble Pd in the liquid samples. This rapid autocatalytic synthesis of metallic Pd^0 had a >99.7% yield, spontaneously coating 11.2 g Pd/m^2 on membranes within 150 minutes.

[0060] Other dose concentrations (0.1 mM, 1 mM, and 5 mM) of Na_2PdCl_4 as the precursor also were tested. The Pd^0 synthesis follow the similar kinetic pattern with the similar >99% yield. FIGs. 3-A1 to 3-D5 show scanning transmission electron microscopy (STEM) images using a range of magnifications of these Pd^0-films. In general, all the Pd^0 anchored on the membranes were nanoparticles of ≤ 5 nm.

2. Application of MCfR: destruction of oxyanions with Pd^0-films

[0061] Precious metal-films in the H_2-MCfR system are able to catalyze reduction of a variety of oxyanions. These oxyanions include but are not limited to: nitrate (NO_3^-), nitrite (NO_2^-), perchlorate (ClO_4^-), chlorate (ClO_3^-), selenate (SeO_4^{2-}), selenite (SeO_3^{2-}), arsenate (AsO_4^{3-}), antimonate ($Sb_2O_7^{4-}$/SbO_4^{3-}), vanadate ($V_2O_7^{4-}$ /VO_4^{3-}), chromate ($Cr_2O_7^{2-}$/CrO_4^{2-}), molybdate ($Mo_2O_7^{2-}$/MoO_4^{2-}), tungstate ($W_2O_7^{2-}$ /WO_4^{2-}), and perrhenate (ReO^{4-}/ReO_5^{3-}).

[0062] FIGs. 4A-4C present selected examples for nitrite reduction (4A), chromate reduction (4B), and chlorate reduction (4C) catalyzed by 0.56 g/m_2 Pd^0-film (0.1 mM Pd precursor) in the H_2-MCfR.

[0063] As shown in FIG. 4A, over 90% of the initial 4 mM (56 mg-N/L) NO_2^- was rapidly removed (within 10 minutes), and the NO_2^- concentration dropped below the MCL (1 mg- N/L) [10] within 15 minutes. The decrease in NO_2^- concentration fit well to a pseudo- first-order decay model (R^2 = 0.989) with an observed catalytic activity of 25.8 $L \cdot g_{Pd}^{-1} \cdot min^{-1}$, a value similar to reported activities of suspended Pd^0 catalysts supported by metal oxides under optimal conditions (4.4 - 48 $L \cdot g_{Pd}^{-1} \cdot min^{-1}$). The rate was almost 100-fold faster than reported for PVP-supported Pd [13]. A transient, but inconsiderable accumulation of N_2O (up to 5% of the total initial N) occurred during the first 10 minutes, followed by fast consumption within 5 minutes). Neither NO nor NH^{4+} was detected throughout the 30-minute test, which gives > 99.9% selectivity towards N_2, the desired product.

[0064] As shown in FIG. 4B, over 90% and 95% of the initial 0.4 mM (20 mg-Cr/L) CrO_4^{2-} was immediately removed within 90 and 120 minutes, respectively. The CrO_4^{2-} concentration eventually dropped below its MCL (0.1 mg-Cr/L) within 150 minutes. The decrease in CrO_4^{2-} concentration fit well to a pseudo-first-order decay model (R_2 = 0.991), with an observed catalytic activity rate of 3.0 $L \cdot g_{Pd}^{-1} \cdot min^{-1}$. The rate was slightly lower than the highest reported values for H_2-induced colloidal or Al_2O_3-supported Pd catalysts (3.6 and 6.7 $L \cdot g_{Pd}^{-1} \cdot min^{-1}$, respectively). As expected, Cr(III), the product of CrO_4^{2-} reduction, accumulated in the form of soluble Cr^{3+} ion under acidic conditions.

[0065] Chemical reduction of ClO_x^- species, though faster than microbial reduction, is still challenging due to a higher activation barrier for electron transfer than other oxyanions. Similar to NO_3^-, monometallic precious metals are not able to catalyze reduction of the most oxidized perchlorate (ClO_4^-), but the less oxidized ClO_3^-. Even for ClO_3^- reduction, monometallic Pd has been proved not the optimal catalyst due to its low catalytic activity. In the basic H_2-MCfR featuring monometallic PdNPs, only 10% of the initial 1 mM ClO_3^- was reduced during the first 120 minutes. The H_2-MCfR was modified by adding 0.1 mM perrhenic acid ($HReO_4$) prior to ClO_3^- reduction. The soluble ReO_4^- was first reduced to Re_2O_5, which was immobilized on the Pd surface. The Re_2O_5 then functioned as an electron shuttle to lower the activation energy for ClO_3^- reduction. With the assistance of Re_2O_5, ClO_3^- reduction reached 88% removal within 120 minutes (FIG. 4C). The resulting catalytic activity of 1.8 $L \cdot g_{Pd}^{-1} \cdot min^{-1}$ was close to the highest levels reported in previous studies using supported Pd-ReO_x, Rh, or Ru NPs in suspension. Along with ClO_3^-, we observed accumulation of no other less oxidized ClO_x^-, and

free chloride ions (Cl^-) were > 96% of the removed ClO_3^-, which confirms that ClO_3^- was substantially reduced to Cl^-, the desired product.

3. Application of MCfR: destruction of organics with Pd^0-films

[0066] Precious metal-film in the MCfR system is capable of catalyzing reduction of a variety of organics, for example, halogenated compounds, nitrated compounds, and unsaturated hydrocarbons.

[0067] FIGs. 5A-5D present selected examples of trichloroethene (TCE) dechlorination and saturation (5A), trichlorofluoroethane (CFC-11) dechlorination and defluorination (5B), 4-nitrophenol (4-NP) nitro-reduction (5C), and 1,3,5-Trinitroperhydro-1,3,5-triazine (RDX) denitration catalyzed by 0.56 g/m^2 Pd-film (0.1 mM Pd precursor) in the MCfR.

[0068] As shown in FIG. 5A, more than 99% of the initial 42 μmole TCE was removed with a pseudo-first-order catalytic activity of 5.4 $L \cdot g_{Pd}^{-1} \cdot min^{-1}$ (R_2 = 0.989), and 97% of the Cl in the initial TCE was released as Cl^- during the 85-minute test. The tests further confirm that, in addition to dechlorination, the membrane-supported PdNPs also were able to catalyze hydrogenation of unsaturated C=C bonds to saturated C-C bonds.

[0069] Among the possible reduced products from TCE, saturated monochloroethane (MCA; 17.4% selectivity) and ethane (82.6% selectivity) accumulated, while unsaturated dichloroethene (DCE, or $C_2H_2Cl_2$) and vinyl chloride (VC, or C_2H_3Cl) were not detected throughout the 85-minute test. This supports that hydrogenating saturation of the C=C bond (H addition) was prior to dechlorination (H replacement) in TCE.

[0070] As shown in FIG. 5B, over 90% and 95% of 50 μM CCl3F was removed within 3 and 4 hours, respectively, at a pseudo-first-order catalytic activity of 1.4 $L \cdot g_{Pd}^{-1} \cdot min^{-1}$ (R_2 = 0.989). The CCl_3F dehalogenation rate in the MCfR at room temperature was faster than any CFC dehalogenation reported at higher temperatures (at least 75°C; usually > 300°C) using noble metals, transient metals, or zeolite catalysts. F^- and Cl^- were released, eventually accounting for 42% and 45% of the total F and Cl in the initial CCl3F, respectively. This confirms that the membrane-supported PdNPs in the H_2-MCfR were capable of simultaneous dechlorination and defluorination of CFCs at ambient temperature.

[0071] As shown in FIG. 5C, 60% of the initial 96 μM 4-nitrophenol was rapidly removed within one-half minute. Extrapolating the half-minute data reveals a pseudo- first-order catalytic activity of 157 $L \cdot g_{Pd}^{-1} \cdot min^{-1}$ (R_2 = 0.98), a value almost equal to the highest-ever-reported highest value (176.4 $L \cdot g_{Pd}^{-1} \cdot min^{-1}$) for carbon-composite-supported PdNP suspension. The main product was 56 μM 4-aminophenol (4-AP), accounting for 98% of the removed 4-

CP, which confirms that the membrane- supported PdNPs in the H_2-MCfR was able to reduce nitro to amino functional groups around the C-N bond. As the reaction proceeded, 4-CP removal and 4-AP accumulation gradually slowed down. After 4 minutes, the 4-AP concentration started to drop. In the end of the 13-minute test, residual 4-AP was only 4 μM, and appearing was 89 μM of 4-aminocyclohexanone, the saturated counterpart of 4-AP. This supports a pattern of 4-NP destruction: C-N reduction followed by C=C saturation. Meanwhile, along with the 4-AP depletion, the retarded 4-nitrophenol removal recovered, reaching 99% and 99.9% within 8 and 12 minutes, respectively. This reveals a new possible trend that was not observed in the 4-CP test: the presence of 4-AP inhibited Pd-catalyzed 4-NP reduction, probably due to competition in adsorption sites. Loss of 4-AP eliminated the competition.

[0072] As shown in FIG. 5D, over 99.5% of the initial 91 μM RDX was removed within one hour at 22°C and neutral pH. The pseudo-first-order catalytic activity was 6.9 $L \cdot g_{Pd}^{-1} \cdot min^{-1}$ (R_2 = 0.994), a catalytic reactivity considerably higher than most photocatalytic and ZVI/Fention processes and close to the recent Bi/Fe^0 or Pd/Fe^0 bimetallic processes. The residual concentration then dropped to below the detection limit (20 μg/L, close to EPA health advisory level) within 90 minutes. We also observed transient accumulation of NO_2^-, but no appearance of less nitrated cyclic intermediates; this indicates that the nitro functional group around the N-N bond in RDX was thoroughly denitrated, and the ring was further cleaved. In addition, the NO_2^- consumption confirmed that PdNPs catalyzed subsequent NO_2^- reduction, and absence of nitrous oxide (N_2O) and ammonium (NH^{4+}) confirms a nearly 100% selectivity towards N_2.

[0073] Table 1 summarizes the reaction pathways and products of Pd-film-catalyzed reduction of the organic contaminants described above as well as other representative organics that have been tested in the MCfR system. The list of the target contaminants in Table 1 is not exhaustive.

4. Application of MCfR: operational condition controls for optimizing catalytic activities and product selectivity

[0074] FIGs. 6A-6H present the reduction of selected oxidized contaminants (nitrite, chlorite, TCE, and 4-CP) catalyzed by the Pd-film with variable conditions (catalyst type, catalyst dosage, pH, and H_2 pressure) that can be conveniently and accurately tuned in the MCfR system.

[0075] Different types of catalysts lead to distinct catalytic pattern and efficiency. For example, the catalytic activity of monometallic Rh for nitrite reduction is only 1/4th of

monometallic Pd-film, but the bimetallic Pd/Rh-film (at a molar ratio of 1:1) shows similar activity of monometallic Pd (FIG. 6A). The pure Pd-film is scarcely able to catalyze chlorate reduction (FIG. 6B).

[0076] Increasing catalyst dosage enhances contaminant removal rate until a threshold is reached. The threshold, also known as the optimal dosage, yields the fastest contaminant removal and the highest catalytic activity. When the catalyst dosage beyond the optimal level, the contaminant removal remains, but the catalytic activity drops; this indicates redundancy of the catalysts. For example, when the Pd-to-nitrite molar ratio was increased from 1:1,000 to 1:400, the pseudo-first-order rate constant of nitrite reduction catalyzed by the Pd-film accordingly increased from 0.05 to 0.25 min^{-1}, and the catalytic activity increased from 15 to 25 L/g-Pd/min. When the Pd dosage further increased to 1:100, the rate constant slightly increased to 0.28 min^{-1}, while the catalytic activity dramatically dropped to 5 L/g-Pd/min (FIG. 6C). It can be concluded that the Pd-to-nitrite ratio of 1:400 was close to the optimal dosage for nitrite reduction catalyzed by the Pd-film in the MCfR system.

[0077] Catalyst dosage not only affects catalytic efficiency but also determines product selectivity. For example, when the molar ratio of Pd to 4-CP was 0.1:1, the product was exclusively phenol when the 4-CP removal reached 99% (Fig. 6D); this indicates that only dechlorination occurred. When the molar ratio of Pd to 4-CP was higher than 1:1, substantial products became the saturated cyclohexanol and phenol was inconsiderable at 99% 4-CP removal (FIG. 6D); this indicates ring saturation, driven by more abundant catalyst, also occurred along with dechlorination. Under this scenario, specific catalyst dosage is designed in order to maximize the catalytic selectivity towards a certain desired product.

[0078] Catalytic reduction of nitrite (FIG. 6E) was considerably faster in acidic conditions than neutral conditions. This is in accord with previous reports that lower pH usually is preferred in reduction reactions catalyzed by precious metals, as anions such as hydroxide (OH^-) and carbonate (CO_3^{2-}), which naturally become more abundant under alkaline conditions, deactivate precious metal catalysts. Furthermore, the reaction of H_2 oxidation coupled with nitrite reduction produces bases that further increase pH. This obstacle, however, can be attenuated by providing acid from CO_2 gas in the MCfR system. In specific, the gas-transfer membranes can deliver multiple gases (for example, H_2 and CO_2) at a desired ratio. For the treatment of neutral-pH water, the nitrite reduction rate was doubled and tripled for 20% and 50% CO_2 supply along with H_2 than for no CO_2 supply (FIG. 6E).

[0079] Higher H_2 pressure means a faster supply of the electron donor and can promote catalytic efficiency. For example, in the MCfR for TCE removal (FIG. 6G), an increase of the

H_2 pressure from 2.5 to 15 psig not only increased catalytic activity by almost four times, but also enhanced the selectivity towards desired nontoxic ethane from 80% to 95%. However, the H_2 pressure needs to be carefully regulated for two reasons: 1) excess H_2 beyond "supply on demand" wastes H_2, which can lead to economic and safety problems; and 2) in some cases, too-rapid H_2 supply leads to selectivity towards undesired products. From example, when the H_2 pressure was higher than 10 psig, undesired ammonium accumulated as a result of over-reduction of nitrite beyond the harmless N_2 gas (FIG. 6F).

5. Application of MCfR: long-term removal of co-existing TCA and TCE catalyzed by Pd^0-film under continuous operation

[0080] The H_2-MCfR system can operate continuously for long-term removal of a sole or multiple oxidized contaminants from water with minimal detachment or deactivation of the precious metal-film catalysts. For example, the H_2-MCfR was continuously fed with water contaminated by TCA and TCE for over 90 days. FIG. 7 presents the operational conditions and effluent results. Tables 2-4 summarizes the average performance results at steady states of nine stages featuring a range of influent TCA/TCE concentrations, H_2 pressures, pHs, and HRTs. Overall, the TCA and TCE removals were substantial during the 90-day operation. When the total surface loading of TCA and TCE was no more than 2 $g/m^2/day$ (Stages I to VII and IX), TCA and TCE removals at steady state were over 96% and 90%, respectively. When the total surface loading was doubled (Stage VIII), the TCA and TCE removals at steady state only moderately decreased, to 89% and 75%, respectively.

[0081] Weekly monitoring of Pd concentrations in the effluent samples reveal that detached Pd^0 from the membrane surface was minimal (6.2 ± 4.4 μg/L). The cumulative catalyst loss during the 90-day operation was 0.16 mg, or only 4% of the total Pd coated on the membrane. These results verify that the MCfR system is capable of long-term treatment of contaminants at high surface loading with minimal loss of the catalyst quantity or quality.

6. Activation of MCfR: forming a Pd/Rh catalyst film

[0082] For a bench-scale MCfR featuring a Pd/Rh-film, the concentration of Pd and Rh in the precious metal medium was 2.5 mM for both metals. FIG. 8 shows the concentration profile of the Pd and Rh species over time in the MCfR. More than 99% of the total Pd ions and Rh ions were converted to Pd^0 and Rh^0 within 180 minutes of exposure to the precious metal medium (pH. Of 7, HRT = 24 hours, H_2 gas provided at 20 psig). The spontaneously coated gas transfer membrane has a loading density of 5.6 g Pd/m^2 and 5.6 g Rh/m^2. FIGs. 9A and 9B

are transmission electron microscopy images of the Pd/Rh-film, which show the Pd nanoparticles and the Rh nanoparticles are formed together, perhaps as alloy catalysts. FIGs. 9C and 9D are electron energy loss spectroscopy images that show the distribution of the Pd and Rh nanoparticles in the catalyst film. The Pd nanoparticles and Rh nanoparticles were distributed homogenously, and the diffraction patterns indicate presence on different planes. Pd^0 is present on four different planes: (1 1 1), (2 0 0), (2 2 0) and (3 1 1). Rh^0 only appears on two planes: (2 0 0) and (4 0 0).

[0083] For a bench-scale MCfR featuring a Pd/Ir-film, the concentration of Pd and Ir in the precious metal medium was 2.5 mM for both metals. Although Ir(IV) cannot be autocatalytically reduced to form Ir^0NPs, Pd^0 catalysis, allowed Ir(IV) to be reduced and form Ir^0 NPs.

7. Application of a bimetallic MCfR: Bimetallic catalyst films can defluorinate PFOA

[0084] The bench-scale MCfRs with the bimetallic catalyst films were run at ambient conditions (23°C and 1 atm) with the influent pH being 7 at HRT of 24 hours. H_2 gas was provided at 20 psig. The results of PFOA and F^- concentrations in a H_2-MCfR with a Pd/Rh-film are shown in FIG. 10A. A 29-hour test with this H_2-MCfR resulted in over 60% of the PFOA was depleted and reductive defluorination (43.8 μM F^- accumulation, accounting for 21.9% of the total F in the ~10 μM PFOA) with a pseudo-zero-order rate of 1.73 μM/h. The results of PFOA and F^- concentrations in a H_2-MCfR with a Pd/Ir-film are shown in FIG. 10B. A 115-hour test with this H_2-MCfR resulted in 99% PFOA depletion with a pseudo-first-order rate of 0.215 h^{-1} with reductive defluorination (124.2 μM F^- accumulation, accounting for 65.2% of the total F in the ~7.6 μM PFOA) with a pseudo-zero-order rate of 1.12 μM/h in the H_2-MPfR during.

[0085] As summarized in FIG. 10C, Pd/Rh-film and Pd^0/Ir^0 showed much higher defluorination rates than mono-Pd^0 and mono-Rh^0. This was caused by the synergistic effect of the bimetallic catalyst. Pd^0 played a key role in adsorbing PFOA and H_2, while Rh^0 was responsible for carbon-fluoride dissociation. The Pd/Ir-film also showed much higher PFOA removal rate than mono-Pd^0 at pH 7.

8. Application of a bimetallic MCfR: Long-term removal of PFOA catalyzed by Pd/Rh-film under continuous operation

[0086] FIG. 11 shows the PFOA concentrations in the influent and effluent of a MCfR with Pd/Rh-film under environmentally relevant concentrations of PFOA during a period of 30 days.

Within the first day of the experiment, the effluent PFOA decreased sharply to <136 μM (or 75% removal). For the following 29 days, the effluent concentration of PFOA stabilized at 82 ± 35 ppt (or 83 ± 8% removal). Thus, bimetallic catalyst films are capable of long-term treatment of contaminants.

Table 1. Organic contaminants catalyzed by Pd-film in the continuous H_2-MCfR.

Target Contaminant		**Catalyst in MCfR**	
Category	**Name**	**Pathway**	**Desired Products**
Herbicide/ Pesticide	Chlorophenols	Dechlorination	Phenol
		Ring saturation	Cyclohexanol
	2,4-dichlorophenoxyacetic acid	Dechlorination	Phenoxyacetic acid
	3,6-dichloro-2-methoxybenzoic acid	Dechlorination	2-methoxybenzoic acid
	1-chloro-3-ethylamino-5-isopropylamino-2,4,6-triazine	Dechlorination	3-ethylamino-5-isopropylamino-2,4,6-triazine
	3,5-dibromo-4-hydroxybenzonitrile	Debromorination	4-hydroxybenzonitrile
Disinfection byproduct	Trichloroacetic acid	Dechlorination	Acetic acid
	Trichloroacetonitrile	Dechlorination	Acetonitrile
	NDMA	Denitration	Dimethylamine
	Bromochloroiodomethane	Dehalogenation	Methane
Solvent	Trichloroethane	Trichloroethane	Ethane
	Trichloroethene	Chloroform	Ethane
		Chain saturation	
	Chloroform	Dechlorination	Methane
Freon	CFC-11	Dechlorination	Methane
	CFC-12	Dechlorination	Methane
	CFC-113	Dechlorination	Ethane
Precursors/ raw materials	Phenol	Ring saturation	Cyclohexanol
	Nitrophenols	Nitro-reduction	Aminophenols
		Ring saturation	Aminocyclohexanols
	PFAS	Defluorination	Nonfluorinated hydrocarbons
Explosive	1,3,5-Trinitro-1,3,5-triazinane	Denitration	hexamethylenetetramine
	1,3,5,7-Tetranitro-1,3,5,7-tetrazoctane	Denitration	1,3,5,7-Tetrazocane
	TNT	Nitro-reduction	2,4,6-Triaminotoluene

Table 2. Average performance results at steady states in the continuous H_2-MCfR (8 mg-Pd/m^2-membrane) with various influent TCA concentration, H_2 pressure, pH, and HRT.

				TCA				
	H_2	**pH**	**HRT**	**C_{in}**	**Surface Loading**	**C_{out}**	**Flux**	**Removal**
Stage	*psig*	*s.u.*	*hour*	*mM*	*g/m^2/d*	*μM*	*g/m^2/d*	*%*
I	**3**	**7**	**6.0**±0.3	0.1	**0.10**±0.02	**11.2**±1.6	**0.09**±0.00	**88.8**±1.6

II	**3**	**7**	**6.2**±0.3	0.5	**0.50**±0.03	**35.8**±6.7	**0.44**±0.01	**92.8**±1.3
III	**3**	**7**	**6.2**±0.4	1	**1.00**±0.07	**173.4**±15.0	**0.93**±0.02	**87.5**±1.5
IV	**6**	**7**	**6.1**±0.3	1	**1.02**±0.05	**89.7**±10.3	**0.92**±0.04	**91.0**±1.0
V	**9**	**7**	**6.2**±0.2	1	**1.00**±0.03	**57.8**±10.0	**0.94**±0.02	**94.2**±1.0
VI	**3**	**4**	**6.0**±0.3	1	**1.03**±0.05	**133.7**±8.1	**0.90**±0.05	**86.8**±0.8
VII	**3**	**11**	**6.2**±0.1	1	**1.0**±0.01	**118.9**±31.6	**0.88**±0.01	**88.1**±2.2
VIII	**3**	**7**	**3.2**±0.2	1	**1.94**±0.07	**251.0**±12.5	**1.45**±0.06	**74.9**±1.2
IX	**3**	**7**	**12.3**±0.2	1	**0.50**±0.03	**51.5**±4.0	**0.48**±0.03	**94.9**±0.4

Table 3. Average performance results at steady states in the continuous H_2-MCfR (8 mg-Pd/m^2-membrane) with various influent TCE concentration

				TCE				
	H_2	**pH**	**HRT**	**C_{in}**	**Surface Loading**	**C_{out}**	**Flux**	**Removal**
Stage	*psig*	*s.u.*	*hour*	*mM*	*g/m^2/d*	*μM*	*g/m^2/d*	*%*
I	**3**	**7**	**6.0**±0.3	0.1	**0.10**±0.01	**0.7**±0.8	**0.10**±0.00	**99.3**±0.8
II	**3**	**7**	**6.2**±0.3	0.5	**0.49**±0.03	**12.5**±2.2	**0.48**±0.00	**97.5**±0.4
III	**3**	**7**	**6.2**±0.4	1	**0.98**±0.07	**36.3**±8.5	**0.95**±0.01	**96.7**±0.9
IV	**6**	**7**	**6.1**±0.3	1	**1.00**±0.05	**27.3**±3.5	**0.97**±0.01	**97.3**±0.4
V	**9**	**7**	**6.2**±0.2	1	**0.98**±0.02	**22.8**±1.4	**0.95**±0.01	**97.7**±0.1
VI	**3**	**4**	**6.0**±0.3	1	**1.02**±0.05	**27.7**±2.6	**0.95**±0.01	**97.2**±0.3
VII	**3**	**11**	**6.2**±0.1	1	**0.98**±0.01	**39.8**±3.2	**0.95**±0.01	**96.0**±0.3
VIII	**3**	**7**	**3.2**±0.2	1	**1.91**±0.07	**112.5**±12.5	**0.95**±0.01	**88.8**±1.3
IX	**3**	**7**	**12.3**±0.2	1	**0.50**±0.03	**12.4**±4.8	**0.49**±0.02	**98.8**±0.5

Table 4. Average DCA, MCA, and ethane selectivity during different stages.

				Selectivity		
	H_2	**pH**	**HRT**	**DCA**	**MCA**	**Ethane**
Stage	*psig*	*s.u.*	*hour*	*%*	*%*	*%*
I	**3**	**7**	**6.0**±0.3	**4.1**±0.8	**1.9**±0.8	**94.0**±0.8
II	**3**	**7**	**6.2**±0.3	**3.1**±0.4	**11.3**±1.1	**85.6**±1.5
III	**3**	**7**	**6.2**±0.4	**2.5**±0.1	**15.3**±1.9	**82.2**±1.8
IV	**6**	**7**	**6.1**±0.3	**1.5**±0.1	**12.6**±1.3	**85.9**±1.5
V	**9**	**7**	**6.2**±0.2	**1.3**±0.1	**10.8**±0.4	**87.9**±0.4
VI	**3**	**4**	**6.0**±0.3	**2.4**±0.2	**14.2**±1.6	**83.4**±1.7
VII	**3**	**11**	**6.2**±0.1	**2.2**±0.1	**14.1**±0.8	**83.7**±0.9
VIII	**3**	**7**	**3.2**±0.2	**6.0**±0.3	**35.0**±3.8	**58.9**±4.0
IX	**3**	**7**	**12.3**±0.2	**2.1**±0.3	**9.5**±0.5	**88.4**±0.6

CLAIMS

What is claimed:

1. A method of establishing a catalyst film for long-term removal of oxidized contaminants from a fluid, the method comprising:

providing a non-porous gas transfer membrane, wherein the non-porous gas transfer membrane comprises a gas-phase side and a liquid-phase side;

contacting the liquid-phase side of the non-porous gas transfer membrane with a precious metal medium, the precious metal medium comprising a precious metal salt and a solvent; and

contacting the gas-phase side of the non-porous gas transfer membrane with hydrogen (H_2) gas at a sufficient partial pressure to convert at least 90% of the precious metal salt in the precious metal medium to an elemental form;

wherein the elemental form of the precious metal is in the form of a nanoparticle and is deposed on the liquid-phase side of the non-porous gas transfer membrane.

2. A method of removing oxidized contaminants from a fluid, the method comprising:

establishing a catalyst film, the catalyst film comprising precious metal nanoparticles on a non-porous gas transfer membrane;

contacting a fluid containing oxidized contaminants with the catalyst film; and

contacting the catalyst film with hydrogen (H_2) gas at a sufficient partial pressure to reduce the oxidized contaminants.

3. The method of claim 2, wherein the step of establishing a catalyst film comprises:

providing the non-porous gas transfer membrane, the non-porous gas transfer membrane comprising a gas-phase side and a liquid-phase side;

contacting the liquid-phase side of the non-porous gas transfer membrane with a precious metal medium, the precious metal medium comprising a precious metal salt and a solvent; and

contacting the gas-phase side of the non-porous gas transfer membrane with H_2 gas at a sufficient partial pressure to convert at least 90% of the precious metal salt in the precious metal medium to elemental form.

4. The method of claim 3, wherein the catalyst film is deposed on the liquid-phase side of the non-porous gas transfer membrane.

5. The method of any one of claims 1-4, wherein the precious metal salt comprises palladium (II).

6. The method of claim 5, wherein the catalyst film consists of precious metal nanoparticles with a mean diameter of less than 5 nm.

7. The method of claim 5, wherein the precious metal salt further comprises rhodium (III), ruthenium (III), or iridium (IV).

8. The method of claim 5, wherein the precious metal salt consists of:
palladium (II),
palladium (II) and rhodium (III),
palladium (II) and ruthenium (III), or
palladium (II) and iridium (IV).

9. The method of any one of claims 1-8, wherein the pH of the precious metal medium is 7 ± 0.5.

10. The method of any one of claims 1-9, wherein the gas-phase side of the non-porous gas transfer membrane is contacted with H_2 gas at a sufficient partial pressure to convert at least 99% of the precious metal in the precious metal medium to elemental form.

11. The method of any one of claims 1-10, wherein the sufficient partial pressure of H_2 gas to convert at least 90% of the precious metal in the precious metal medium to elemental form is 10 ± 1 psig.

12. The method of any one of claims 1-11, wherein the concentration of the precious metal in the precious metal medium is 0.1-5 mM.

13. The method of claim 12, wherein the concentration of the precious metal in the precious metal medium is 0.1 ± 0.01 mM, 1 ± 0.1 mM, 2 ± 0.2 mM, or 5 ± 0.5 mM.

14. The method of any one of claims 1-13, wherein the solvent is selected from the group consisting of: water, salt solution, hydrochloric acid, methanol, ethanol, acetonitrile, toluene, dichloromethane, chloroform, and tetrahydrofuran.

15. A system for removing oxidized contaminants from a fluid, the system comprising:
a non-porous gas transfer membrane;
a catalyst film comprising precious metal nanoparticles; and
a hydrogen (H_2) gas source,
wherein:
the catalyst film is deposed on the non-porous gas transfer membrane;
the precious metal nanoparticles and the H_2 gas are configured to catalyze the reduction of oxidized contaminants; and
the oxidized contaminants are at least one member selected from the group consisting of: nitrite, chromate, chlorate, trichloroethene, trichloroethane, nitrophenol, RDX, and perfluorooctanoate.

16. The system of claim 15, wherein the non-porous gas transfer membrane comprises a gas-phase side and a liquid-phase side, the catalyst film is deposed on the liquid-phase side and the H_2 gas source delivers H_2 gas to the gas-phase side.

17. The system of claim 15 or 16, wherein the precious metal nanoparticles comprise a platinum group metal.

18. The system of claim 17, wherein the catalyst film consists of precious metal nanoparticles with a mean diameter of less than 5 nm.

19. The system of claim 17, wherein the precious metal nanoparticles consist of:
palladium,
palladium and rhodium,
palladium and ruthenium, or
palladium and iridium.

20. The system of any one of claims 15-19, wherein the non-porous gas transfer membrane is a hollow-fiber membrane.

21. The system of claim 20, wherein the hollow-fiber membrane with a wall thickness 50-55 μm.

22. The system of claim 20 or 21, wherein the outer diameter of the hollow-fiber membrane is 200 μm and/or the inner diameter of the hollow-fiber membrane is 100-110 μm.

23. The system of any one of claims 15-22, wherein the non-porous gas transfer membrane is made of a polymeric material selected from the group consisting of: polypropylene, polyurethane, polysulfone, and composite forms.

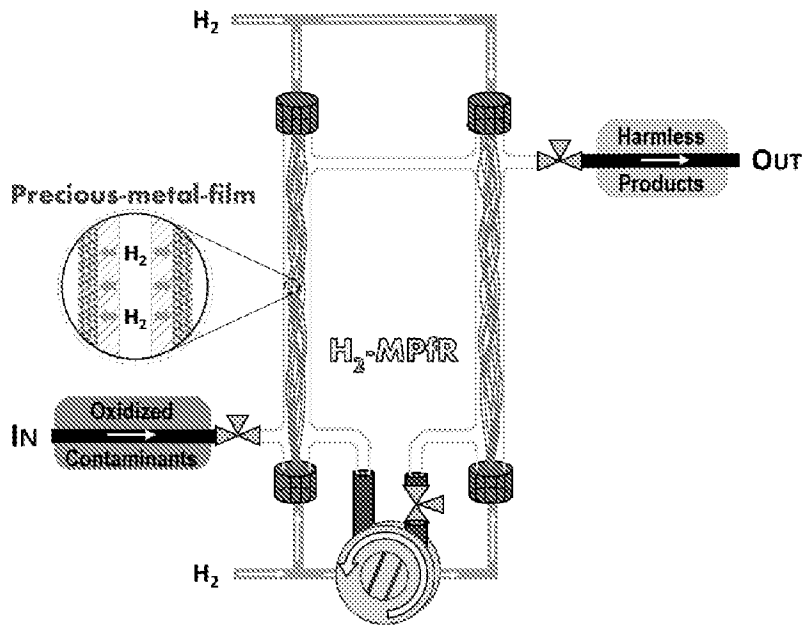

H2
Harmless
Products
OUT
Precious-metal-film
H2
H2
H2-MPfR
IN
Oxidized
Contaminants
H2

FIG. 1

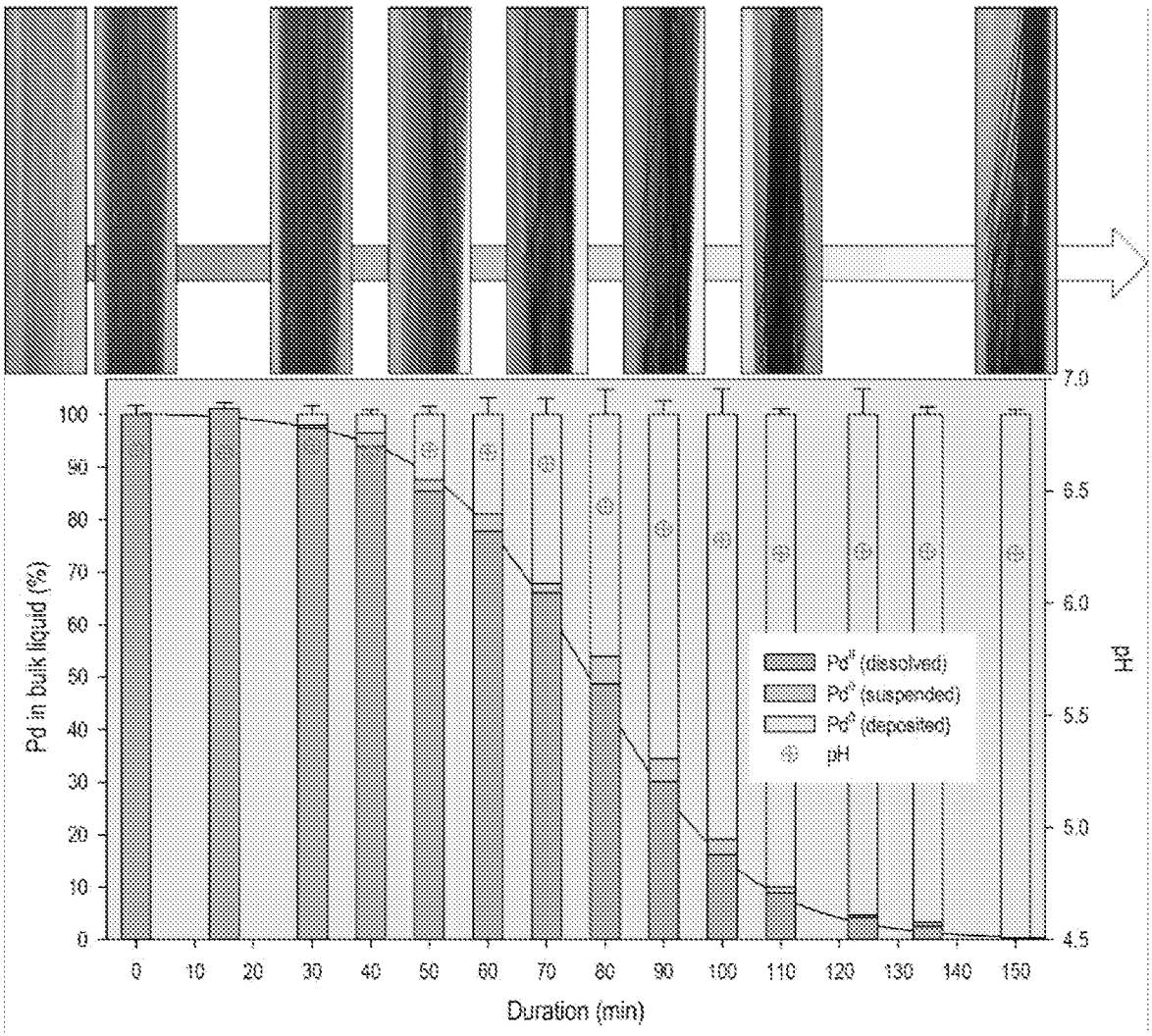

Pd in bulk liquid (%)
pH
Duration (min)
Pd^{II} (dissolved)
Pd^{0} (suspended)
Pd^{0} (deposited)
pH

FIG. 2

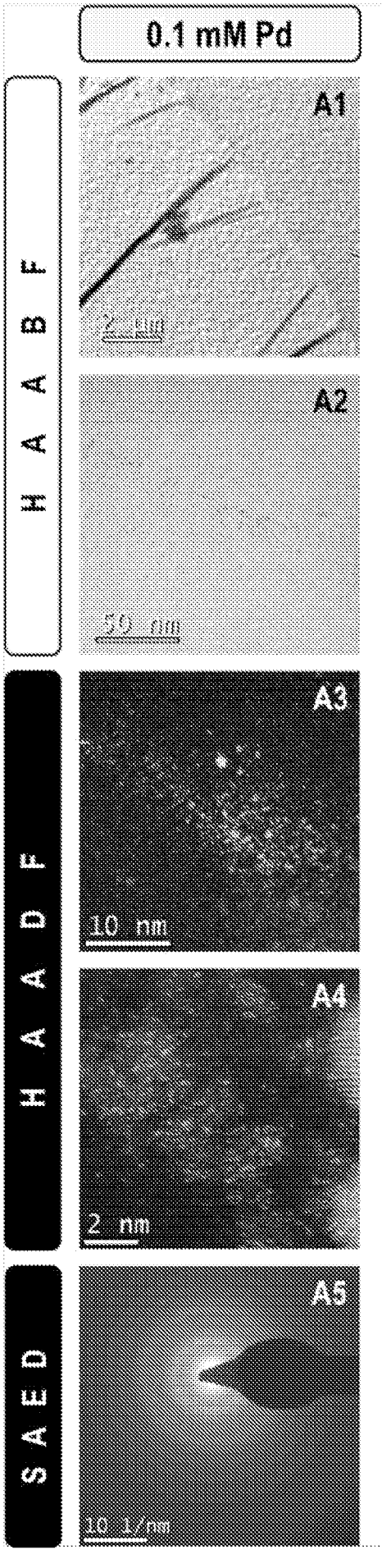


FIG. 3-A1

FIG. 3-A2

FIG. 3-A3

FIG. 3-A4

FIG. 3-A5

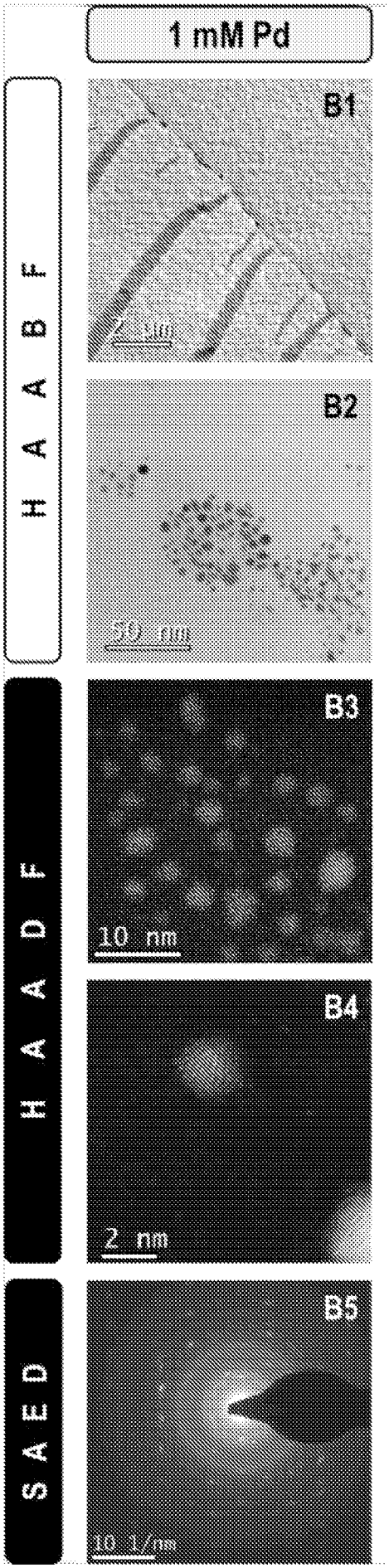


FIG. 3-B1

FIG. 3-B2

FIG. 3-B3

FIG. 3-B4

FIG. 3-B5

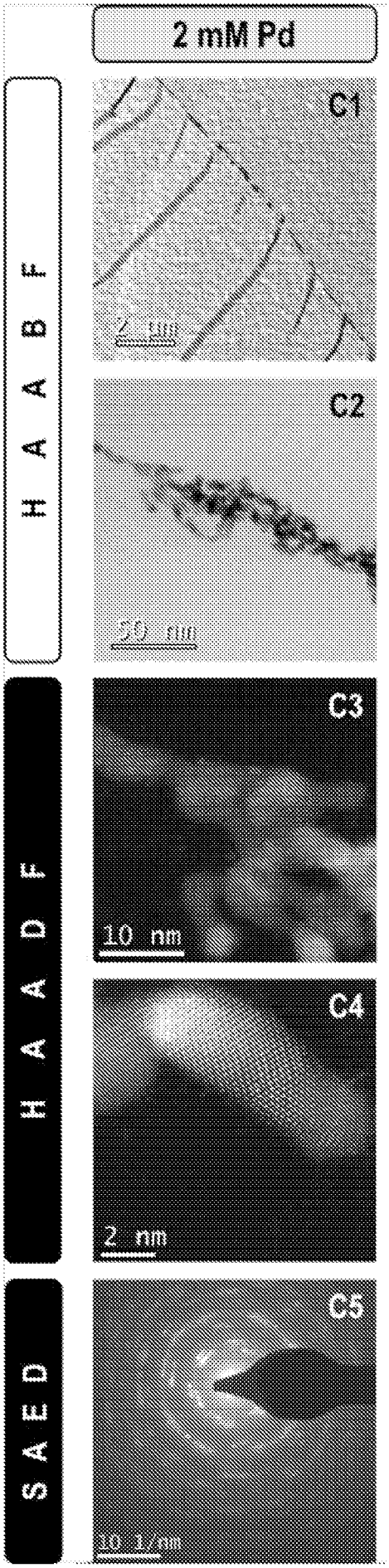


FIG. 3-C1

FIG. 3-C2

FIG. 3-C3

FIG. 3-C4

FIG. 3-C5

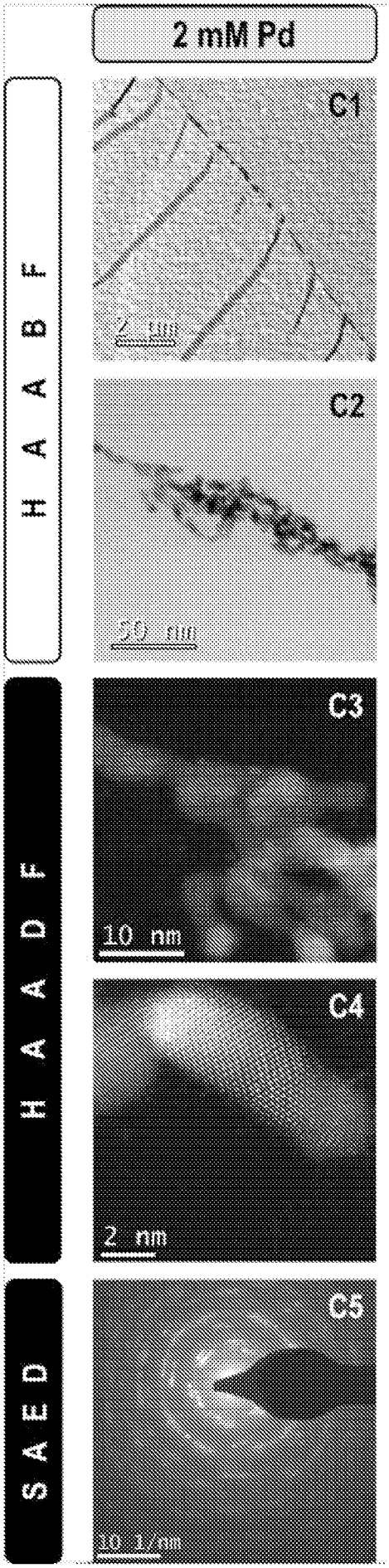


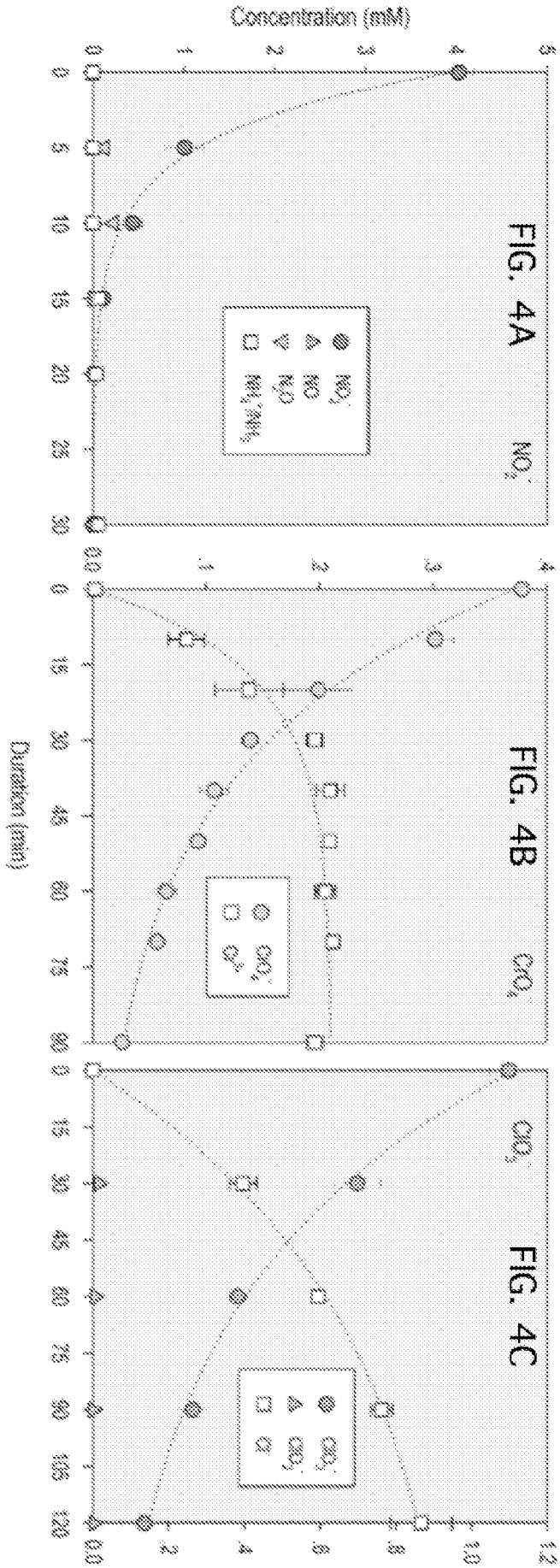
FIG. 3-D1

FIG. 3-D2

FIG. 3-D3

FIG. 3-D4

FIG. 3-D5


Concentration (mM)
Duration (min)
FIG. 4A
FIG. 4B
FIG. 4C

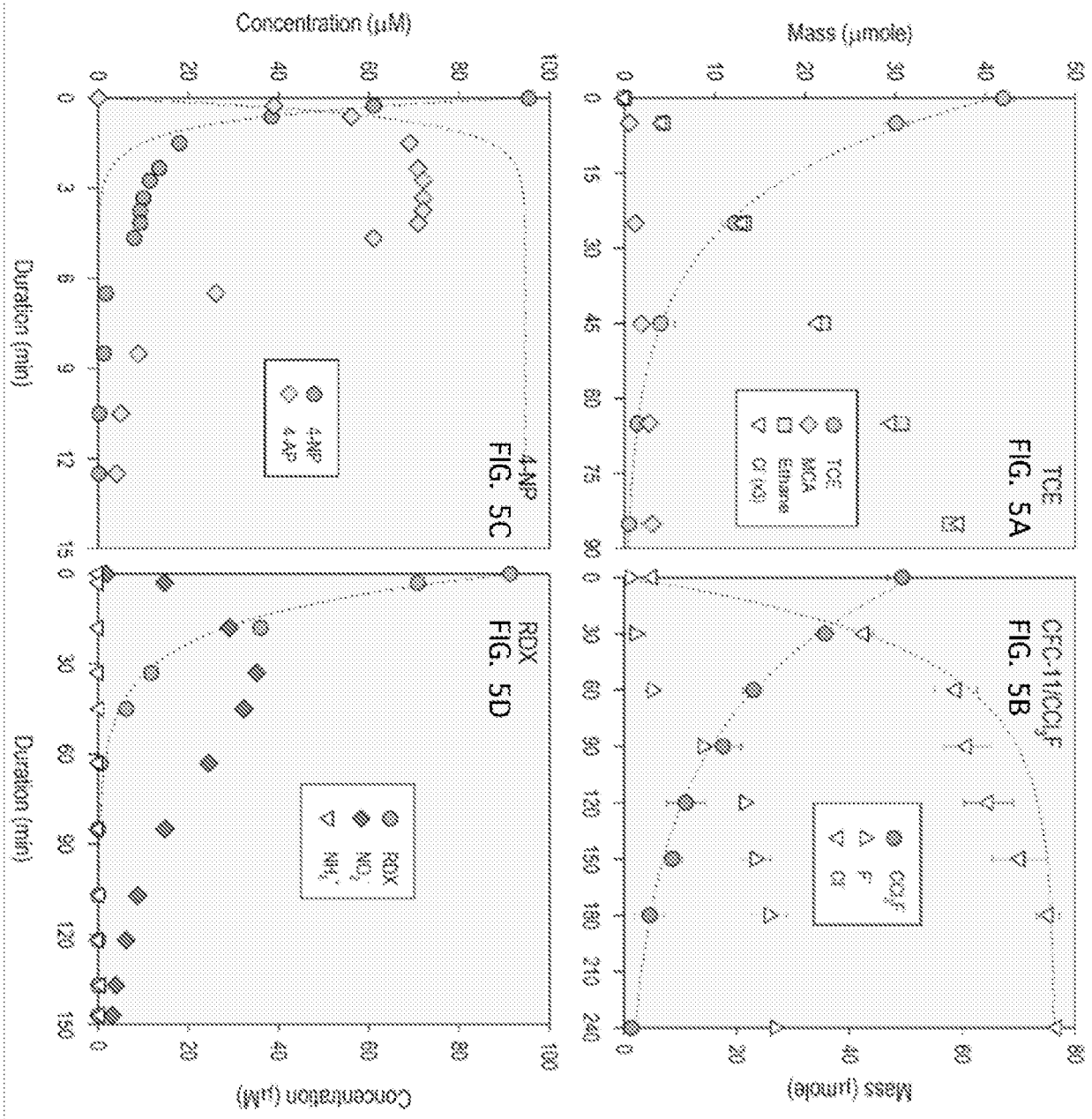

Mass (μmole)
Duration (min)
TCE
TCE
MCA
Ethane
CH4
FIG. 5A
Mass (μmole)
Duration (min)
CFC-11 (CCl_3F)
CCl_3F
F
Cl
FIG. 5B
Concentration (μM)
Duration (min)
4-NP
4-NP
4-AP
FIG. 5C
Concentration (μM)
Duration (min)
RDX
RDX
NO_3^-
NH_4^+
FIG. 5D

FIG. 6A

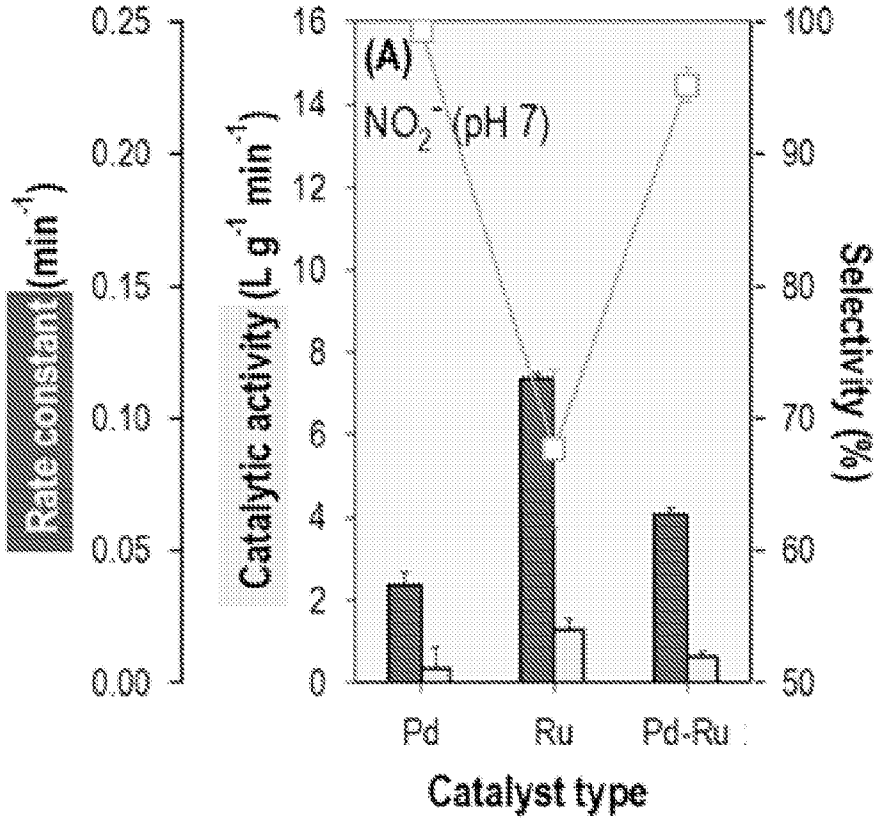

(A)
NO_2^- (pH 7)
Rate constant (min^{-1})
Catalytic activity ($L\ g^{-1}\ min^{-1}$)
Selectivity (%)
0.25
0.20
0.15
0.10
0.05
0.00
16
14
12
10
8
6
4
2
0
100
90
80
70
60
50
Pd
Ru
Pd-Ru
Catalyst type

FIG. 6B

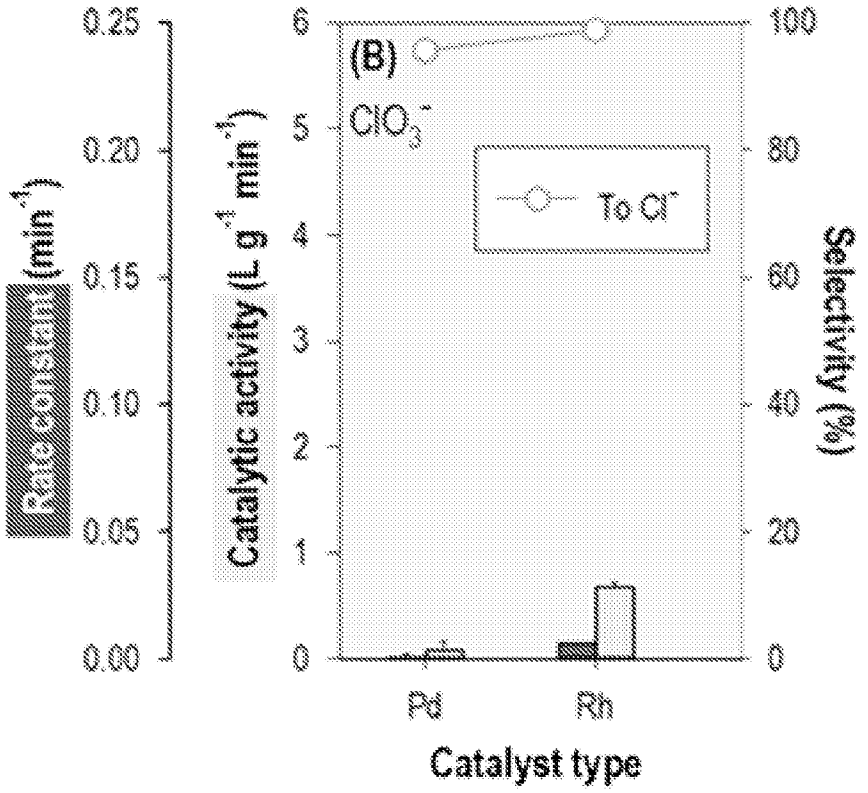

(B)
ClO_3^-
To Cl^-
Rate constant (min^{-1})
Catalytic activity ($L\ g^{-1}\ min^{-1}$)
Selectivity (%)
0.25
0.20
0.15
0.10
0.05
0.00
6
5
4
3
2
1
0
100
80
60
40
20
0
Pd
Rh
Catalyst type

FIG. 6C

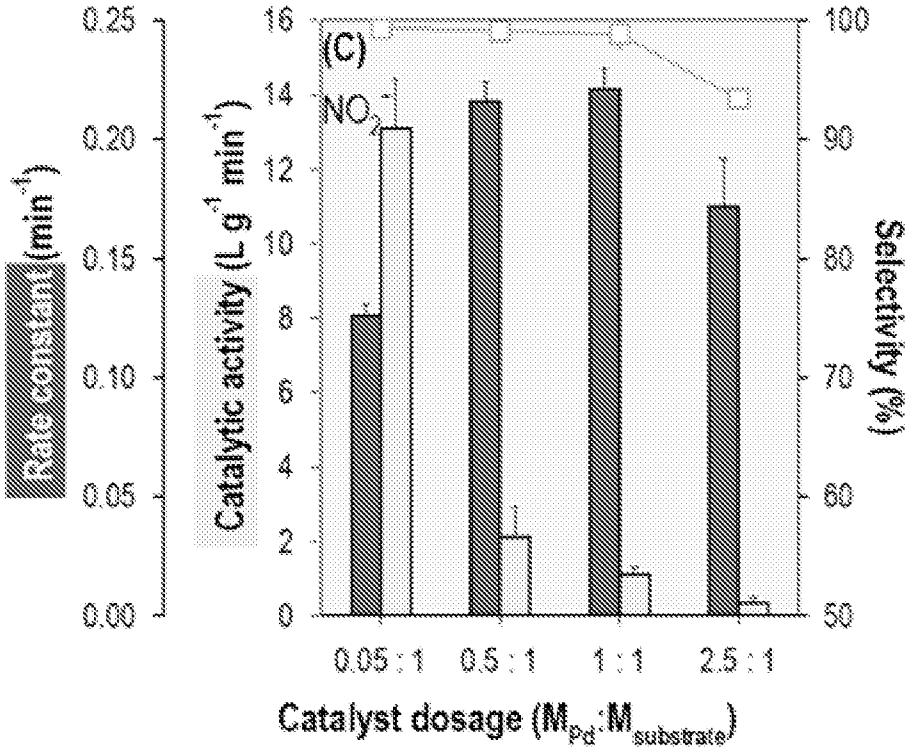

(C)
NO_2
Rate constant (min^{-1})
Catalytic activity (L g^{-1} min^{-1})
Selectivity (%)
0.05 : 1
0.5 : 1
1 : 1
2.5 : 1
Catalyst dosage (M_{Pd}:$M_{substrate}$)

FIG. 6D

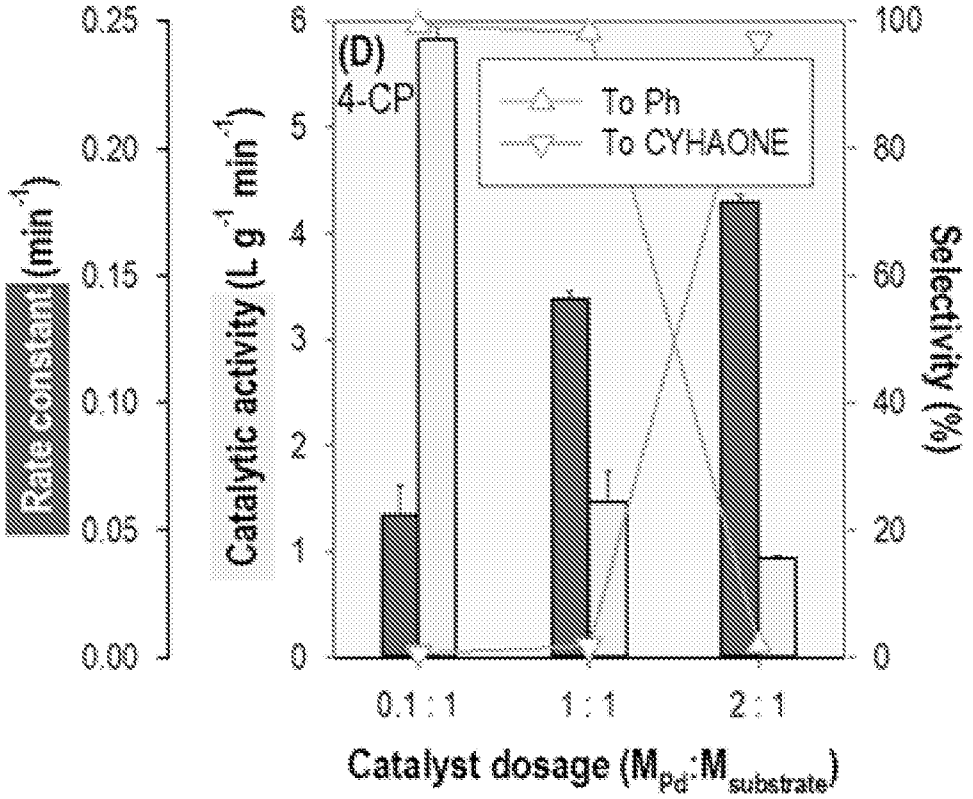

(D)
4-CP
To Ph
To CYHAONE
Rate constant (min^{-1})
Catalytic activity (L g^{-1} min^{-1})
Selectivity (%)
0.1 : 1
1 : 1
2 : 1
Catalyst dosage (M_{Pd}:$M_{substrate}$)

FIG. 6E

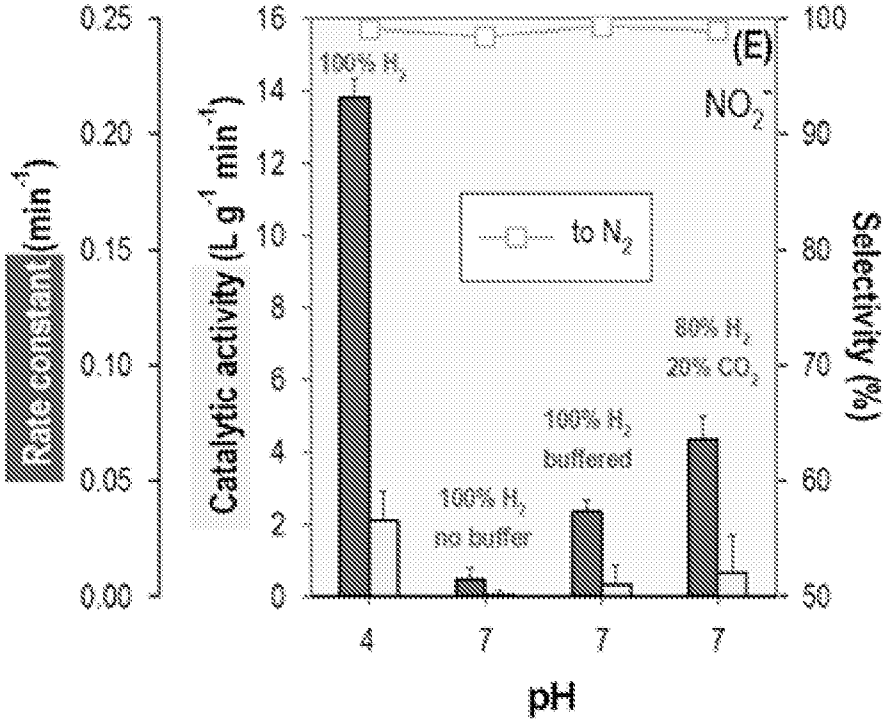

Rate constant (min^{-1})
Catalytic activity (L g^{-1} min^{-1})
Selectivity (%)
(E)
NO_2^-
100% H_2
to N_2
80% H_2
20% CO_2
100% H_2
buffered
100% H_2
no buffer
pH
4
7
7
7

FIG. 6F

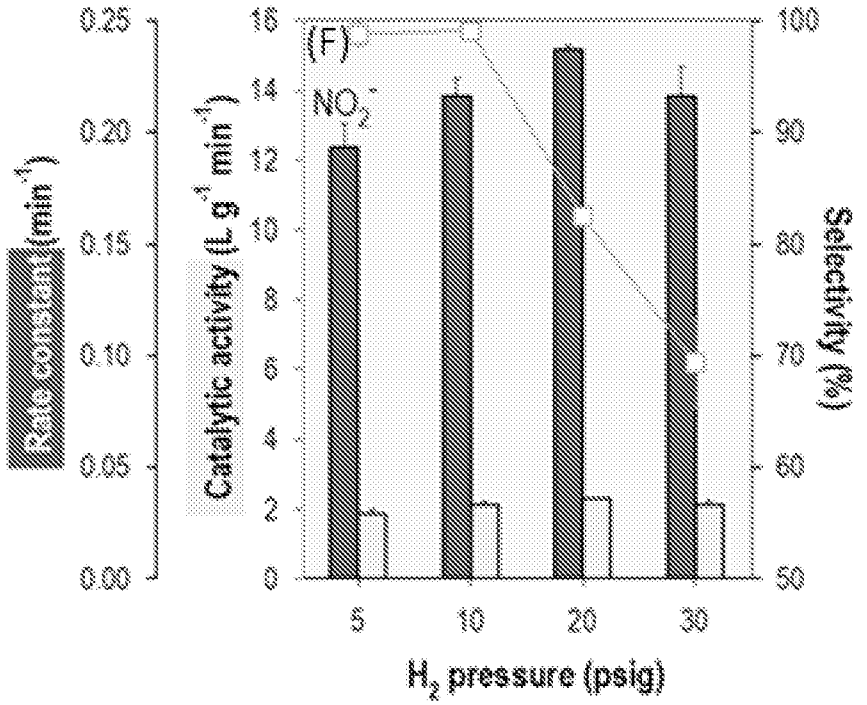

Rate constant (min^{-1})
Catalytic activity (L g^{-1} min^{-1})
Selectivity (%)
(F)
NO_2^-
H_2 pressure (psig)
5
10
20
30

FIG. 6G

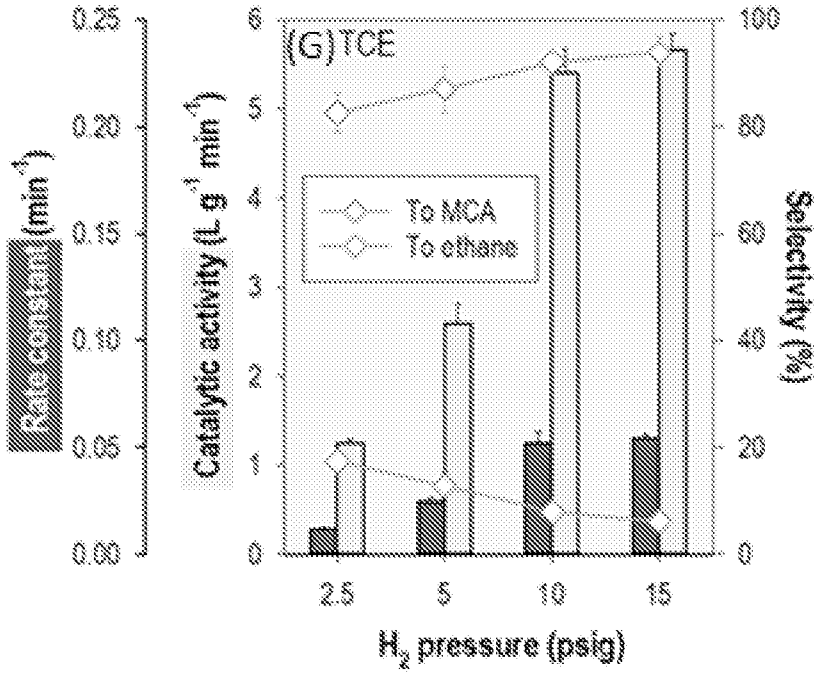

(G)TCE
To MCA
To ethane
Rate constant (min-1)
Catalytic activity (L g-1 min-1)
Selectivity (%)
H2 pressure (psig)
0.25
0.20
0.15
0.10
0.05
0.00
6
5
4
3
2
1
0
100
80
60
40
20
0
2.5
5
10
15

FIG. 8

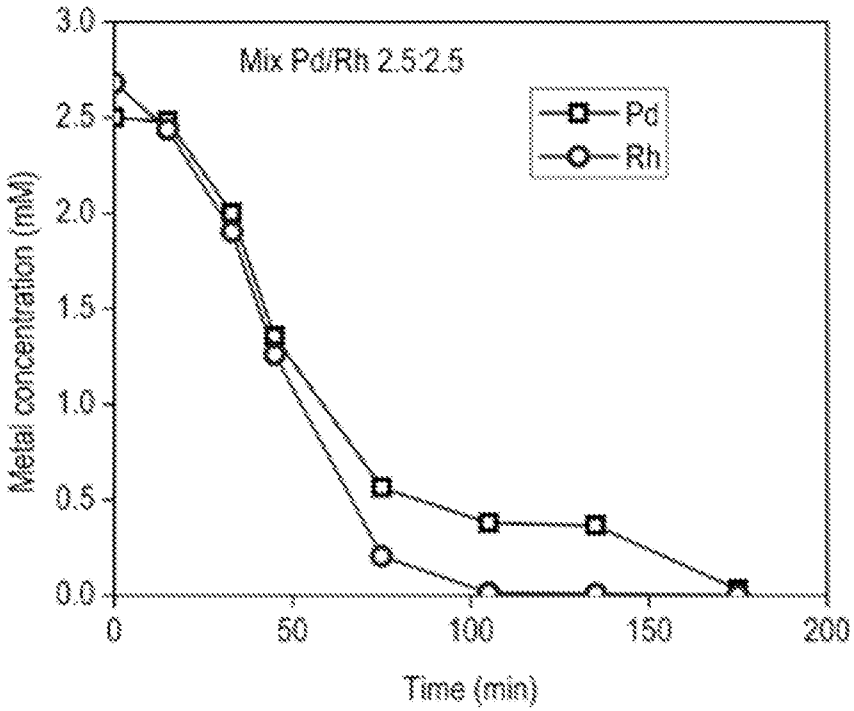
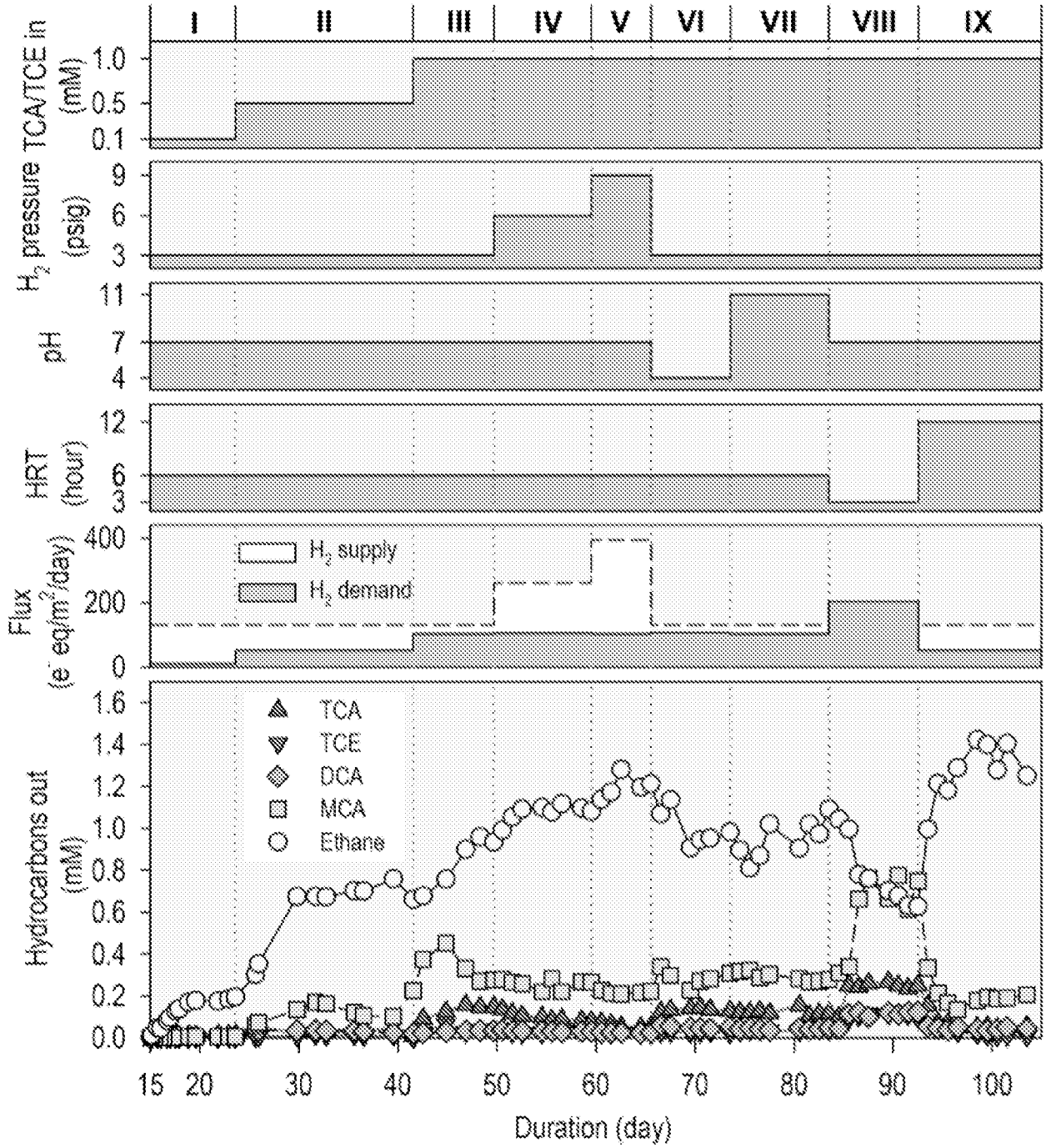
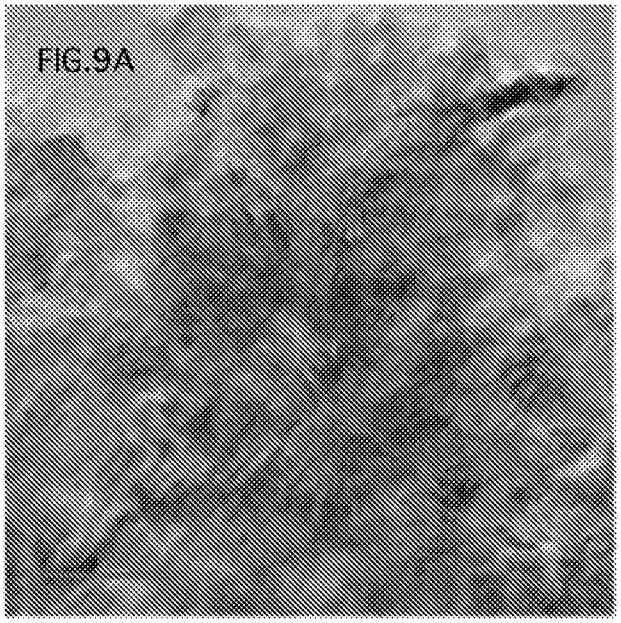
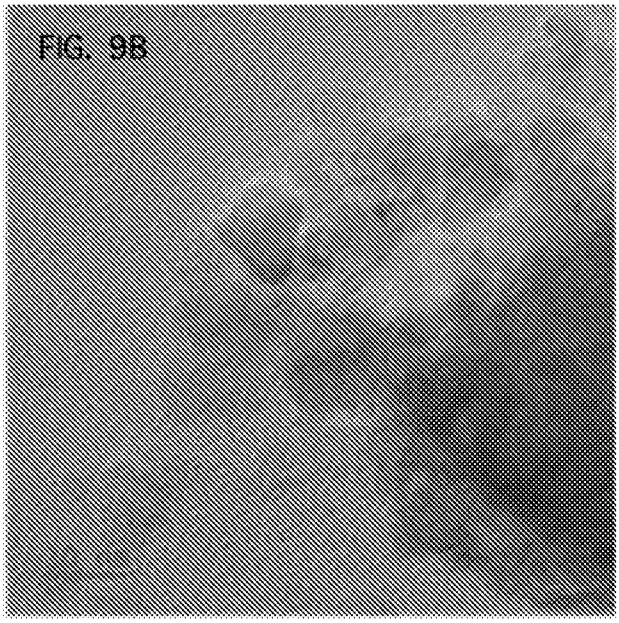
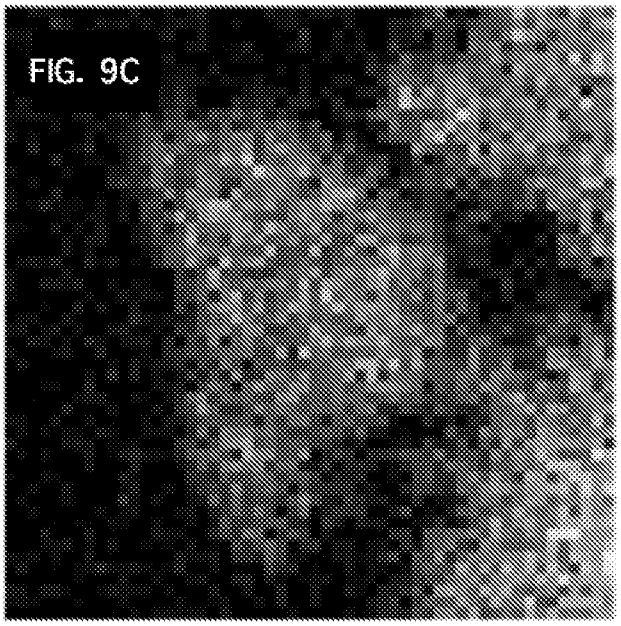

Mix Pd/Rh 2.5:2.5
Pd
Rh
Metal concentration (mM)
Time (min)
3.0
2.5
2.0
1.5
1.0
0.5
0.0
0
50
100
150
200

FIG. 7


I
II
III
IV
V
VI
VII
VIII
IX
TCA/TCE in (mM)
1.0
0.5
0.1
H2 pressure (psig)
9
6
3
pH
11
7
4
HRT (hour)
12
6
3
Flux (e- eq/m2/day)
400
200
0
H2 supply
H2 demand
Hydrocarbons out (mM)
1.6
1.4
1.2
1.0
0.8
0.6
0.4
0.2
0.0
TCA
TCE
DCA
MCA
Ethane
15
20
30
40
50
60
70
80
90
100
Duration (day)


FIG.9A


FIG. 9B


FIG. 9C

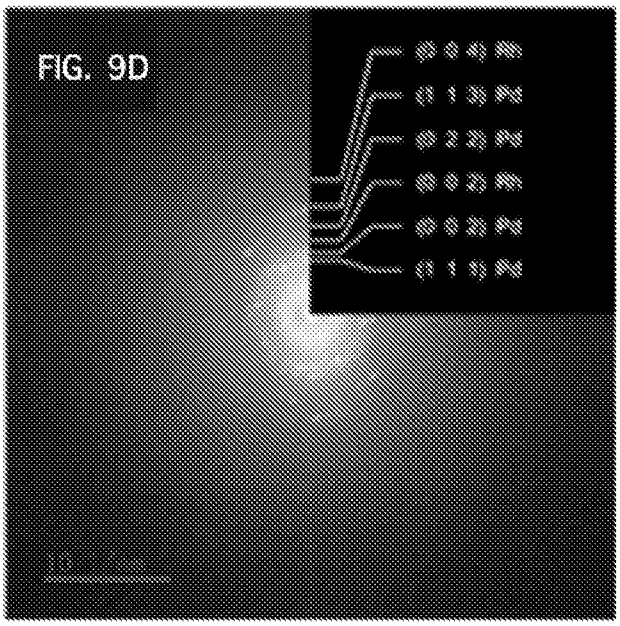

FIG. 9D

FIG. 10A

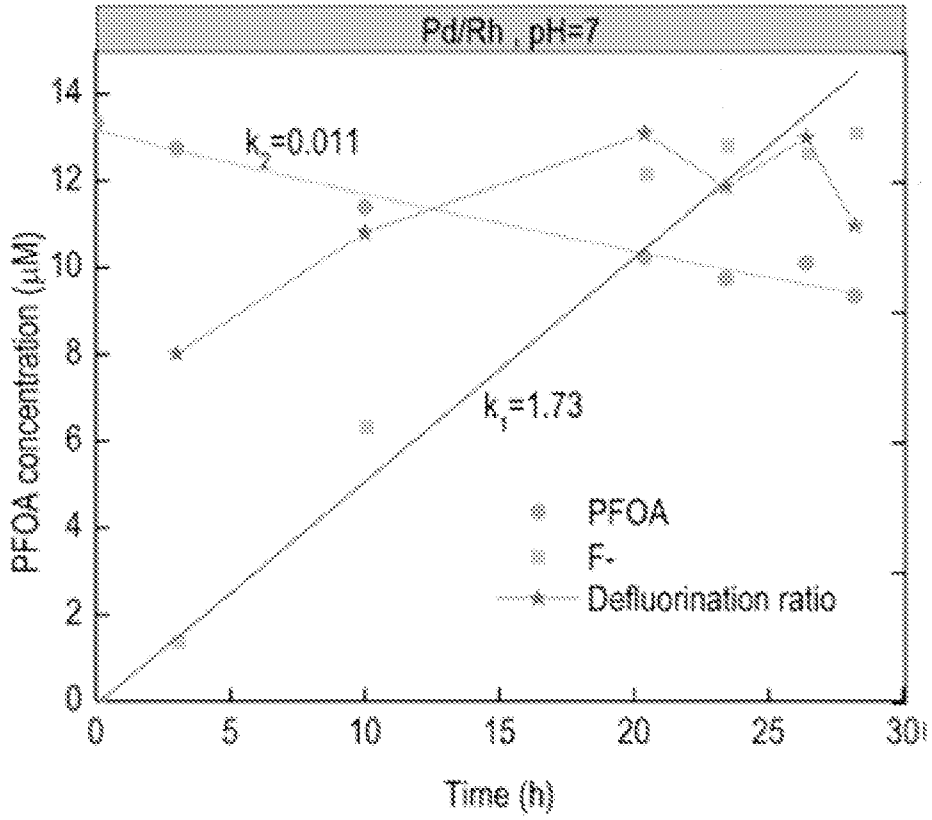


FIG. 10B

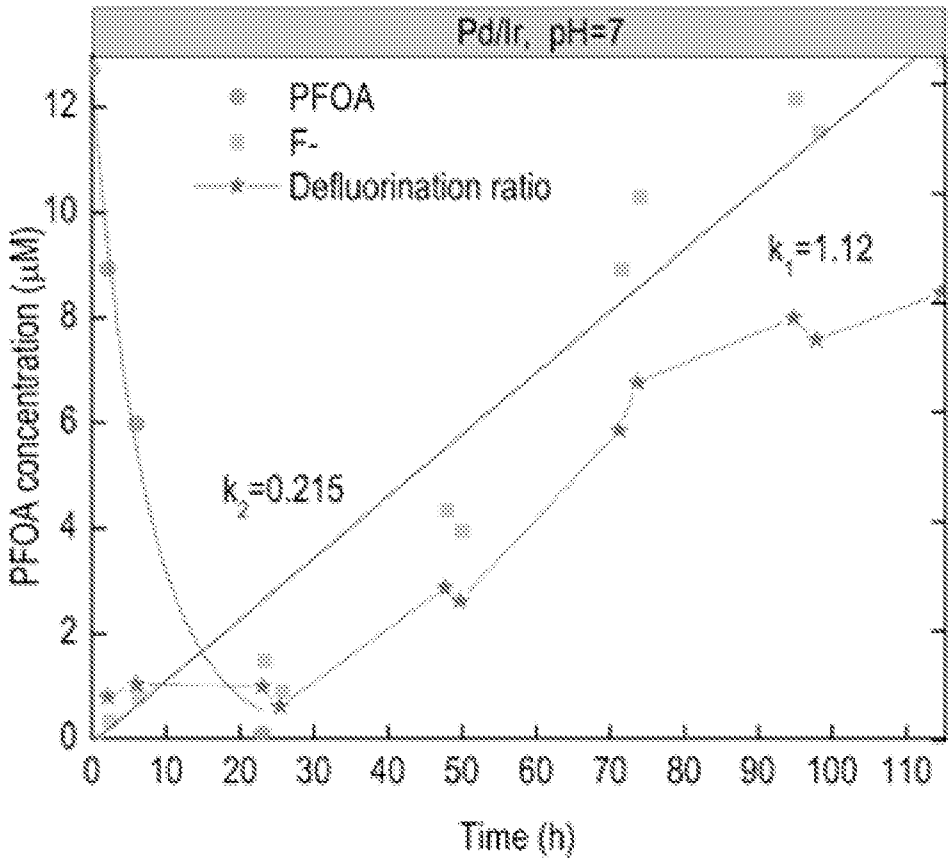


FIG. 10C

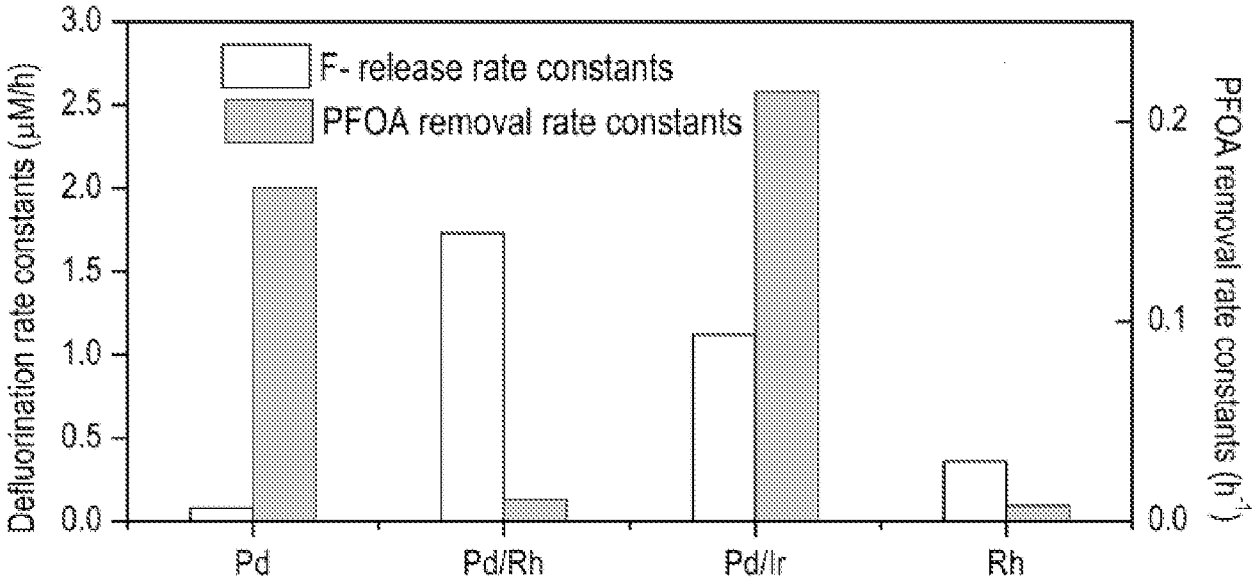


FIG. 11

